

Lorentz-equivariant flow with four delays of neutral type

Jayme De Luca^a

^a*Departamento de Física, Universidade Federal de São Carlos, São Carlos, São Paulo
13565-905, Brazil*

Abstract

We generalize electrodynamics with a second interaction in lightcone. The time-reversible equations for two-body motion define a semiflow in $C^2(\mathbb{R})$ with four state-dependent delays of neutral type and nonlinear gyroscopic terms. Furthermore, if the initial segment includes velocity discontinuities, their propagation requires two energetic Weierstrass-Erdmann continuity conditions as the constraints defining the boundary layer neighborhoods of large velocities and small denominators. Finally, we discuss the motion restricted to a straight line and a fixed one-dimensional segment with vanishing accelerations.

Keywords: neutral differential-delay equations, state-dependent delay, ODEs, and semiflows.

1. Introduction

A. *Significance of the problem and contents*

Variational electrodynamics possess neutral differential-delay equations of motion (NDDE) with state-dependent delays [1–3]. A hindrance to integrating a NDDE forward like an ordinary differential equation (ODE) is the non-invertibility of the linear form containing the most advanced accelerations. Here we cure the non-invertibility by adding a specific Lorentz-invariant term to the action functional. For the two-body problem, the equation of motion is a NDDE with four state-dependent **delays**, which can be integrated like an ODE, using, for example, the MATLAB function **ddensd**. A variational principle is an economical way to derive time-reversible Lorentz-equivariant models possessing differential-delay equations of motion free of divergencies. Some important details to keep in mind are

1. NDDEs are semiflows on infinite-dimensional spaces [4–7]. Unlike ODEs, the initial condition for a NDDE is a **trajectory segment**.

Email address: jayme.deluca@gmail.com (Jayme De Luca)

Preprint submitted to Journal of Differential Equations

April 22, 2022

2. The NDDEs studied here can start even from trajectory segments possessing **only two** derivatives. For example, the acceleration segment can be given by the Takagi-van der Waerden function. The velocity will be the integral of the continuous acceleration, thus belonging to $C^1(\mathbb{R})$. Orbital segments of $C^2(\mathbb{R})$ with accelerations that are only continuous and nowhere differentiable are henceforth referred to as *serrated* orbits.
3. At the expense of satisfying two Weierstrass-Erdmann energetic constraints, and in order to avoid head-on collisions, the initial segment *should* include velocity discontinuities caused by collisions-at-a-distance. The largest initial-condition set of orbital segments with a countable number of velocity discontinuities is the set of continuous segments possessing two derivatives **piecewise**, i.e., $\hat{C}^2(\mathbb{R}) \subset \hat{C}^\infty(\mathbb{R})$.
4. Trajectory termination by the particles crashing *at the speed of light* is a perceived difficulty of electromagnetic modeling even when starting from trajectory segments belonging to $C^\infty(\mathbb{R})$, e.g., the one-dimensional two-body problem with attractive interaction[8]. We perturb electrodynamics with an interaction in lightcone having one control parameter ε and in a way that preserves Lorentz-equivariance. The head-on instability is prevented by collisions-at-a-distance inside thin boundary layers even if ε is small, thus preserving electrodynamics in large orbital portions.
5. According to [9], a Lorentz-invariant functional with interactions in lightcone has only three interaction terms; (i) the electromagnetic term, (ii) a second term henceforth called the ε -strong interaction and proven here to yield a semiflow for any $\varepsilon \neq 0$, and (iii) the gravity-like term of [9], which was left out for simplicity.
6. Our extension is henceforth called ε -strong variational electrodynamics and abbreviated to ε -**VE**, which reduces to variational electrodynamics for $\varepsilon = 0$ [1, 3, 10]. Electrodynamics is **not** a semiflow on $C^2(\mathbb{R})$, which is why the orbits studied in [11] are C^∞ and the orbits of Refs. [12, 13] had to be studied as a boundary-value problem. Our extension yields a semiflow for any $\varepsilon \neq 0$, which is essential to integrate the dynamics like an ODE using the method of steps.
7. NDDEs can propagate velocity discontinuities. In ε -**VE**, breaking points are required to be inside thin boundary layers where near-luminal velocities are reached and velocity denominators are small [1-3]. Velocity discontinuities are instrumental to avoid head-on collisions in a motion with attractive interaction; all C^∞ -smooth initial segments lead to head-on collisions **at the speed of light**[8], which is never a *globally-low-velocity* orbit[8]. The only way to avoid falling into the proton at the speed of light is to use initial segments with discontinuities. The same is true for the tri-dimensional motion because of the exponential instabilities of the circular orbits [14].

B. How this paper is divided

In §2 and in the caption of Fig. 1 we explain our notation for indices, introduce the lightcone condition and state the multi-purpose Lemma 2.1 about velocity denominators. In §2-A, we introduce the Lorentz-invariant functional of $\varepsilon\text{-VE}$. In Fig. 2, we illustrate the data for the boundary-value problem. Theorem 2.1 is an inequality to estimate the parameter region of electromagnetic dominance. In §2-B, we state the critical point conditions and define some quantities to be used throughout the paper. In §2-C, we put the time-reversible Euler-Lagrange equations of motion. In §2-D, we outline the Weierstrass-Erdmann extremum conditions for minimizers with discontinuous velocities. In §3, in the caption of Fig. 3 we explain the method of steps. In §3-A, we discuss the reconstruction of the most advanced acceleration. In §3-B, we discuss the rank deficiency that prevents electrodynamics to be a semiflow. In §3-C, we write the full NDDE for numerical integration by the method of steps and prove theorem 3.1 on a semigroup property when $\varepsilon \neq 0$. In §3-D, we discuss the motion restricted to a straight line by the initial condition and derive the NDDE for numerical integration by the method of steps. §3-D ends with theorem 3.2 exhibiting a one-parameter fixed-segment for the method of steps in a model for the neutron. Our §3-E is designed to guide future experiments with numerical calculations and discusses domains of initial segments for the method of steps. In §4, we discuss the forward continuation of velocity discontinuities; §4-A has three lemmas about an a priori continuation of the partial-momentum sector of the Weierstrass-Erdmann conditions, i.e., Lemmas 4.1, 4.2 and 4.3. In §4-B, we discuss the over-determination by the (energetic) Weierstrass-Erdmann conditions, which are two scalar conditions defining the collisional boundary layer neighborhood of the breaking point. In §5, we discuss the straight-line motion and classify some collisions-at-a-distance in Lemmas 5.1, 5.2 and 5.3 to be used in a perturbation theory. In §6, we put the discussions and conclusion. The appendix is made of four small subsections; §7-A describing the action of the one-dimensional Lorentz group, §7-B has the outer-cone Lemma 7.1 on the optimality of mutual-recoil collisions-at-a-distance, §7-C has a formula to include an external electromagnetic field in the equations of motion, and last, §7-D discusses the implications of having a semiflow for any non-zero ε , which *qualitative* feature is essential to integrate the NDDE by the method of steps. §7-D discusses the generic element of $C^2(\mathbb{R})$ represented by orbits which **do not** possess any derivative beyond the second derivative, as indicated by the name *serrated*. Theorem 7.1 shows that a non-zero ε allows the serrated orbital segments to be solutions of our NDDE.

2. Lorentz-invariant functional with one control parameter

Our notation for sub-indices is **character-sensitive**, as follows: the greek-letter sub-index α designates charges in general, and, when specified, $\alpha = e$ denotes the electronic quantities and $\alpha = p$ denotes the protonic quantities. The speed of light is $c \equiv 1$ in our unit system, and the electronic charge and electronic mass are $e_e \equiv -1$ and $m_e \equiv 1$, respectively. The quantities (e_p, m_p) are arbitrary in our flexible setup. To describe the repulsive electromagnetic problem one can take $e_p < 0$ and arbitrary m_p . The proton is described in our unit system by using $m_p = M_p \simeq 1837$ and $e_p = 1$. We adopt an inertial frame where every point has a time t defined by Einstein synchronization, and spatial coordinates $\mathbf{x} \equiv (x, y, z) \in \mathbb{R}^3$ such that $(t, x, y, z) \in \mathbb{R}^4$. The two-body problem has coordinates $(t_p, x_p, y_p, z_p, t_e, x_e, y_e, z_e) \in \mathbb{R}^4 \times \mathbb{R}^4$ and we present the equations of motion by giving the derivatives of the (three) spatial coordinates of each particle respect to its time t_α , for $\alpha \in (e, p)$. An **orbit** of the two-body problem is a pair of twice-differentiable functions $(\mathbf{x}_e(t_e), \mathbf{x}_p(t_p)) \in C^2(\mathbb{R})$ and satisfying the equations of motion, i.e., $\mathbf{x}_\alpha : t_\alpha \in \mathbb{R} \rightarrow (x_\alpha, y_\alpha, z_\alpha) \in \mathbb{R}^3$, $\alpha \in (e, p)$, while each $\mathbf{x}_\alpha(t_\alpha)$ is called the **trajectory** of charge α . Orbits with discontinuous velocities in a countable set are studied in the class of continuous functions possessing two derivatives piecewise, henceforth $\hat{C}^2(\mathbb{R})$. Our notation becomes character-sensitive when sewing chains are involved, as illustrated in Figure 1. The former convention is adapted to display formulas involving one charge *and* the past *and* the future positions in lightcone of the other charge, in which case the sub-indices are chosen as three consecutive roman characters taken from (s, k, i, j) in the former order, to denote the sewing chain illustrated in Fig. 1.

Our theory is sensible for trajectories possessing a velocity with a modulus smaller than the speed of light $c \equiv 1$ almost everywhere, i.e.,

$$\|\mathbf{v}_\alpha\| < 1, \quad \alpha \in (e, p), \quad (1)$$

henceforth subluminal trajectories. For orbits satisfying (1), the **lightcone conditions** are defined by

$$t_\alpha = t_i \pm \|\mathbf{x}_i - \mathbf{x}_\alpha(t_\alpha)\| \equiv t_i \pm r_{\alpha i}(t_i, \mathbf{x}_i), \quad (2)$$

for $\alpha \in (k, j)$, where double bars stand for the \mathbb{R}^3 norm. In Ref [3] we show that for orbits belonging to $\hat{C}^2(\mathbb{R})$ and satisfying (1), each sign of the implicit condition (2) has a unique solution defining continuous and twice differentiable maps $t_\alpha(t_i, \mathbf{x}_i) : \mathbb{R} \times \mathbb{R}^3 \rightarrow \mathbb{R}$ and $r_{\alpha i}(t_i, \mathbf{x}_i) : \mathbb{R} \times \mathbb{R}^3 \rightarrow \mathbb{R}$ for $\alpha \in (k, j)$ (illustrated in Fig. 1), where

$$r_{\alpha i}(t_i, \mathbf{x}_i) \equiv \|\mathbf{x}_i - \mathbf{x}_\alpha(t_\alpha)\| = |t_i - t_\alpha|. \quad (3)$$

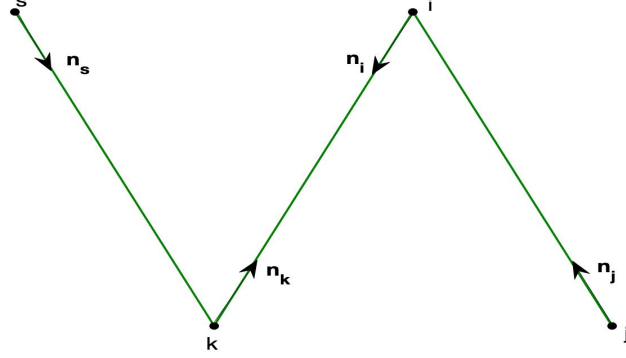


Figure 1: Illustration of the $(skij)$ convention and the unit vectors emanating from the respective positions. When used in the equation of motion for the proton at point i , the past electronic position is at point k while the future electronic position is at point j . On the other hand, for the equation of motion of the electron at point k , the past protonic position is at point s while the future protonic position is at point i .

In Ref. [3] we show that the time-in-lightcone t_α and the inter-particle distance $r_{\alpha i}$ defined respectively by (2) and (3) satisfy

$$\frac{\partial t_\alpha}{\partial \mathbf{x}_i}(t_i, \mathbf{x}_i) = \pm \nabla_i r_{\alpha i}(t_i, \mathbf{x}_i) = \frac{\pm \mathbf{n}_\alpha}{(1 \pm \mathbf{n}_\alpha \cdot \mathbf{v}_\alpha)}, \quad (4)$$

where

$$\mathbf{n}_\alpha \equiv \frac{(\mathbf{x}_i - \mathbf{x}_\alpha)}{r_{\alpha i}}. \quad (5)$$

The upper sign in (4) holds when $\alpha = j$, while the lower sign holds when $\alpha = k$. The denominators of (4) are henceforth called *velocity denominators*, which introduce a singularity in the equations of motion derived next. Several quantities in this paper involve the denominator $(1 \pm \mathbf{n}_\alpha \cdot \mathbf{v}_\beta)$, which is non-zero for subluminal orbits. The following Lemma defines a ubiquitous quotient that is finite for subluminal orbits, even in the limit when $\|\mathbf{v}_\beta\| \rightarrow 1$, which is a useful regularization for the numerical calculations.

Lemma 2.1. *For an arbitrary unit direction $\mathbf{n}_\alpha \in \mathbb{R}^3$ and $\|\mathbf{v}_\beta\| < 1$ we have*

$$\frac{(1 - \mathbf{v}_\beta^2)}{(1 - (\mathbf{n}_\alpha \cdot \mathbf{v}_\beta)^2)} \leq 1. \quad (6)$$

Proof. Using the Pythagora's theorem, $\mathbf{v}_\beta^2 = (\mathbf{n}_\alpha \cdot \mathbf{v}_\beta)^2 + \|\mathbf{n}_\alpha \times \mathbf{v}_\beta\|^2$, the left-hand side of (6) can be expressed as

$$\frac{(1 - \mathbf{v}_\beta^2)}{(1 - (\mathbf{n}_\alpha \cdot \mathbf{v}_\beta)^2)} = \frac{(1 - \mathbf{v}_\beta^2)}{(1 - \mathbf{v}_\beta^2) + \|\mathbf{n}_\alpha \times \mathbf{v}_\beta\|^2}. \quad (7)$$

The denominator on the right-hand side of (7) is equal or greater than the numerator, and it is non-zero because $(1 - \mathbf{v}_\beta^2) > 0$ for sub-luminal orbits. \square

A. Lorentz-invariant functional

Here we introduce the Lorentz-invariant functional defined by integration over the infinite-dimensional boundary data and trajectory segments of Fig. 2. The most general Lorentz-invariant functional with interactions in lightcone has only three interaction terms [9]. Our generalization of electrodynamics uses the action written in Ref. [9] with renamed coefficients. After some inspection, one finds that the first term in equation 47 of Ref. [9] is not needed to yield a semiflow, so its coefficient was set to zero for simplicity. The coefficient of the electromagnetic sector is set to the usual product of the charges. Essential for a semiflow on $C^2(\mathbb{R})$ is the third term of the functional in equation 47 of Ref. [9], henceforth called the ε -strong interaction. We chose the third coefficient to be the parameter $\varepsilon \in \mathbb{R}$, yielding our Lorentz-invariant functional for minimization,

$$\begin{aligned} \mathcal{A}_\varepsilon \equiv & - \sum_{\alpha=e,p} \int_{H_B} m_\alpha \sqrt{1 - \mathbf{v}_\alpha^2} dt_\alpha - e_e e_p \int_{H_B} \delta(s_{ep}^2) (1 - \mathbf{v}_e \cdot \mathbf{v}_p) dt_e dt_p \\ & - \varepsilon \int_{H_B} \delta(s_{ep}^2) \sqrt{1 - \mathbf{v}_e^2} \sqrt{1 - \mathbf{v}_p^2} dt_e dt_p, \end{aligned} \quad (8)$$

where $\mathbf{v}_\alpha \equiv \frac{d\mathbf{x}_\alpha}{dt}|_{t_\alpha}$ is the cartesian velocity of particle $\alpha \in (e, p)$ at time t_α and $s_{ep}^2(t_e, t_p)$ is the Lorentz-invariant four-separation defined as a function of two times $s_{ep}^2 : \mathbb{R} \times \mathbb{R} \rightarrow \mathbb{R}$ by

$$s_{ep}^2(t_e, t_p) = (t_e - t_p)^2 - r_{ep}^2(t_e, t_p), \quad (9)$$

where

$$r_{ep} \equiv \|\mathbf{x}_p(t_p) - \mathbf{x}_e(t_e)\|, \quad (10)$$

is the interparticle distance as a function of two times, and the double bars in (10) stand for the \mathbb{R}^3 norm, as always in this manuscript. Still in Eq. (8), the dot represents the scalar product of \mathbb{R}^3 , the integration variables are the particle times and the double integration is to be carried over the trajectory segments and boundary histories defined in Fig. 2 and indicated by H_B . The lightcone condition is the condition $s_{ep}^2(t_e, t_p) = 0$, and in the following we use the standard delta-function identity of summation over the zeros of the argument (e.g. see chapter 14 of Ref. [16]) to integrate (8) over t_e with a fixed t_p , yielding

$$\delta(s_{ep}^2(t_p, t_e)) = \sum_{\mathfrak{z}=\pm 1} \frac{\delta(t_e - t_p \mp \mathfrak{z}r_{ep})}{\left| \frac{\partial s_{ep}^2}{\partial t_e} \right|_{t_e=t_p \pm r_{ep}}} = \frac{\delta(t_e - t_p - r_{ep})}{2r_{ep}(1 + \mathbf{n}_e \cdot \mathbf{v}_e)} + \frac{\delta(t_e - t_p + r_{ep})}{2r_{ep}(1 - \mathbf{n}_e \cdot \mathbf{v}_e)}, \quad (11)$$

where \mathbf{n}_e is defined by Eq. (5) with $i = p$ and $\alpha = e$. In the denominators of (11) and henceforth, r_{ep} is the distance in lightcone as a function of time t_p only, and the plus sign goes when the electronic position is in the future lightcone of t_p , i.e.,

$t_e = t_p + r_{ep}$, while the minus sign goes when the electronic position is in the past lightcone of t_p , i.e., $t_e = t_p - r_{ep}$. We notice that $\delta(s_{ep}^2(t_p, t_e))$ can be expressed by an alternative formula obtained from (11) by exchanging e and p , which should be used when one is integrating over t_p to derive the electronic partial Lagrangian.

Observations; (i) because of Lemma 2.1, our functional (8) is well defined in the domain $\mathcal{D}_{\text{Peano}}$ of trajectory pairs where the denominators of (8) are Lebesgue integrable, i.e.,

$$\mathcal{D}_{\text{Peano}} \equiv \left\{ (\Gamma_e, \Gamma_p) \in C^2(\mathbb{R}) \mid \int \frac{dt_\ell}{r_{\ell j}(1-\mathbf{v}_\ell^2)} < \infty ; \int \frac{dt_j}{r_{ji}(1-\mathbf{v}_i^2)} < \infty \right\}, \quad (12)$$

named after the Cauchy-Peano theorem for ODEs and (ii) the history sets to be used as boundary data for the variational formulation are illustrated in red in Fig. 2 below.

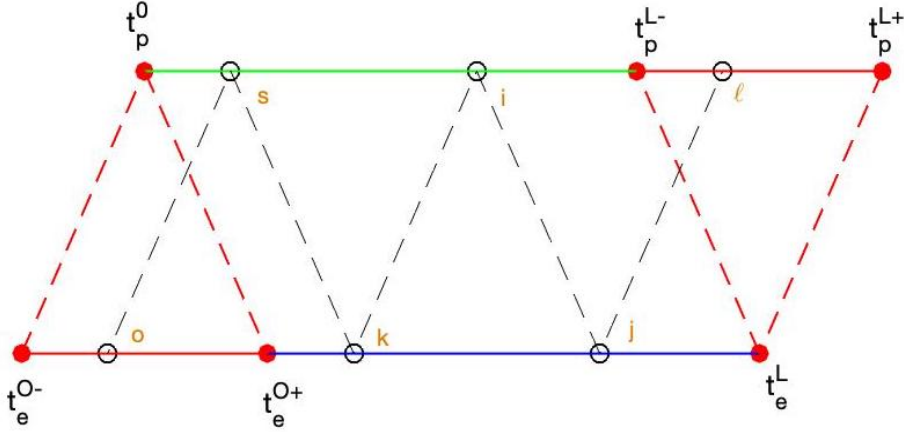


Figure 2: The boundary datum includes the protonic position at the initial time t_p^O , and the continuous and \hat{C}^2 electronic trajectory in (t_e^{O-}, t_e^{O+}) (lower red segment), which interval has endpoints in lightcone with the protonic position at the initial time t_p^O . At the other end, the boundary data include the electronic position at the end time t_e^L , and the continuous \hat{C}^2 protonic trajectory on (t_p^{L-}, t_p^{L+}) (upper solid red segment), which interval is inside the lightcone of the electronic position at the end time t_e^L . The continuous \hat{C}^2 trajectories have two continuous derivatives at every point but a countable set of points along sewing chains of breaking points. Trajectory information on the above boundary data plus trajectory segments, henceforth referred to as the boundary chain H_B , is enough to formulate the variational problem. Illustrated in gold is a sewing chain of particle positions in lightcone, (o, s, k, i, j, l) , and the dashed black lines indicate the lightcones.

In order to define the region of electromagnetic dominance, we show next that the electromagnetic interaction dominates the ε -strong interaction of (8) when $|\varepsilon| < 1$.

Theorem 2.1. *For arbitrary $(\mathbf{v}_p, \mathbf{v}_e) \in \mathbb{R}^3$ with $|\mathbf{v}_p| \leq 1$ and $|\mathbf{v}_e| \leq 1$, we have*

$$\Delta_{ep} \equiv (1 - \mathbf{v}_e \cdot \mathbf{v}_p)^2 - (1 - \mathbf{v}_p^2)(1 - \mathbf{v}_e^2) \geq 0. \quad (13)$$

Proof. The proof is simple and proceeds by re-arranging Eq. (13), yielding

$$\begin{aligned} \Delta_{ep} &\equiv (1 - \mathbf{v}_e \cdot \mathbf{v}_p)^2 - (1 - \mathbf{v}_e^2)(1 - \mathbf{v}_p^2) \\ &= \mathbf{v}_e^2 + \mathbf{v}_p^2 - 2\mathbf{v}_e \cdot \mathbf{v}_p + (\mathbf{v}_e \cdot \mathbf{v}_p)^2 - \mathbf{v}_e^2 \mathbf{v}_p^2 \\ &= (|\mathbf{v}_e| - |\mathbf{v}_p|)^2 + 2(|\mathbf{v}_e||\mathbf{v}_p| - \mathbf{v}_e \cdot \mathbf{v}_p) + (\mathbf{v}_e \cdot \mathbf{v}_p)^2 - \mathbf{v}_e^2 \mathbf{v}_p^2 \\ &= (|\mathbf{v}_e| - |\mathbf{v}_p|)^2 + 2|\mathbf{v}_e||\mathbf{v}_p|(1 - \cos(\theta)) \left(1 - |\mathbf{v}_e||\mathbf{v}_p| \cos^2\left(\frac{\theta}{2}\right)\right) \geq 0, \end{aligned}$$

where θ is the angle between vectors \mathbf{v}_e and \mathbf{v}_p . □

B. Critical point conditions

Minimization of (8) poses two conditions: (i) Euler-Lagrange equations along the piecewise C^2 segments of each trajectory and (ii) the Weierstrass-Erdmann conditions at the breaking points of each trajectory [1, 2]. The critical point of (8) when $i = p$ is obtained by varying the protonic trajectory while fixing its endpoints and its history segments, and fixing the electronic trajectory. The partial Lagrangian of particle $i = p$ is obtained by integrating the double integrals of (8) once over the domain of t_e ; the delta function picks the two zeros of $s_{ep}^2(t_e, t_p)$ when t_e varies, which define the two lightcones. Using (11) to integrate (8) over t_e yields a Lagrangian minimization to find $\min\{\int_{t_O}^{t_L} \mathcal{L}_i(t_i, \mathbf{x}_i(t_i), \mathbf{v}_i(t_i)) dt_i\}$ for

$$\mathcal{L}_i(t_i, \mathbf{x}_i, \mathbf{v}_i) \equiv \mathcal{K}_i - \sum_{\alpha=k,j} e_i (\mathcal{U}_i - \mathbf{v}_i \cdot \mathbf{A}_i) - \varepsilon \sqrt{1 - \mathbf{v}_i^2} \mathbf{G}_i, \quad (14)$$

with \mathcal{K}_i , \mathcal{U}_i , \mathbf{A}_i and \mathbf{G}_i given by

$$\mathcal{K}_i \equiv m_i (1 - \sqrt{1 - \mathbf{v}_i^2}), \quad (15)$$

$$\mathbf{A}_i \equiv \frac{e_k \mathbf{v}_k}{2r_{ki}(1 - \mathbf{n}_k \cdot \mathbf{v}_k)} + \frac{e_j \mathbf{v}_j}{2r_{ji}(1 + \mathbf{n}_j \cdot \mathbf{v}_j)}, \quad (16)$$

$$\mathcal{U}_i \equiv \frac{e_k}{2r_{ki}(1 - \mathbf{n}_k \cdot \mathbf{v}_k)} + \frac{e_j}{2r_{ji}(1 + \mathbf{n}_j \cdot \mathbf{v}_j)}, \quad (17)$$

$$\mathbf{G}_i \equiv \frac{\sqrt{1 - \mathbf{v}_k^2}}{2r_{ki}(1 - \mathbf{n}_k \cdot \mathbf{v}_k)} + \frac{\sqrt{1 - \mathbf{v}_j^2}}{2r_{ji}(1 + \mathbf{n}_j \cdot \mathbf{v}_j)}, \quad (18)$$

where $\mathbf{v}_k \equiv d\mathbf{x}_k/dt|_{t=t_k}$ is the electronic velocity evaluated on the past lightcone and $\mathbf{v}_j \equiv d\mathbf{x}_j/dt|_{t=t_j}$ is the electronic velocity on the future lightcone. Notice

that $\mathcal{K}_i, \mathcal{U}_i, \mathbf{A}_i$ and \mathbf{G}_i are functions of (t_i, \mathbf{x}_i) by Eqs. (2) and (3). Equation (14) defines the protonic partial Lagrangian, while the electronic partial Lagrangian is obtained from (14) by exchanging $(kij) \rightarrow (ski)$ in Eq. (14), i.e., replacing i with k and restricting the summation to the nearest neighbors $\alpha \in (s, i)$ of particle k on the sewing chain of Fig. 1. Observations; (i) unlike the principle of minimal action of classical mechanics, the boundary segments used in Fig. 2 are **infinite-dimensional** [12, 13] and (ii) the procedure explained above yields a different partial Lagrangian for each particle. If the partial Lagrangians were the same, like in classical mechanics, our definition (8) of variational electrodynamics would clash with the no-interaction theorem of Lorentz-equivariant dynamics [15].

C. Euler-Lagrange equations of motion

The Euler-Lagrange equations for particle i on the $\widehat{C}^2(\mathbb{R})$ segments are

$$(m_i + \varepsilon \mathbf{G}_i) \left(\frac{\mathbf{a}_i}{\sqrt{1 - \mathbf{v}_i^2}} + \frac{(\mathbf{v}_i \cdot \mathbf{a}_i) \mathbf{a}_i}{(1 - \mathbf{v}_i^2)^{3/2}} \right) = \frac{1}{2} e_i \sum_{\alpha=k, j} (\mathbf{E}_{\alpha i} + \mathbf{v}_i \times \mathbf{B}_{\alpha i}) - \varepsilon \sqrt{1 - \mathbf{v}_i^2} \left(\nabla \mathbf{G}_i + \gamma_i^2 \frac{d\mathbf{G}_i}{dt_i} \mathbf{v}_i \right), \quad (19)$$

with

$$\mathbf{E}_{\alpha i} \equiv e_\alpha \left(\frac{(1 - \mathbf{v}_\alpha^2)(\mathbf{n}_\alpha \pm \mathbf{v}_\alpha)}{r_{\alpha i}^2 (1 \pm \mathbf{n}_\alpha \cdot \mathbf{v}_\alpha)^3} + \frac{\mathbf{n}_\alpha \times ((\mathbf{n}_\alpha \pm \mathbf{v}_\alpha) \times \mathbf{a}_\alpha)}{r_{\alpha i} (1 \pm \mathbf{n}_\alpha \cdot \mathbf{v}_\alpha)^3} \right), \quad (20)$$

$$\mathbf{B}_{\alpha i} \equiv \mp \mathbf{n}_\alpha \times \mathbf{E}_{\alpha i}, \quad (21)$$

representing, respectively, the other particle's electric and the magnetic fields. When $\alpha = k$ the other particle is in the past lightcone position and the lower sign applies. Otherwise, when $\alpha = j$ the other particle is in the future lightcone position and the upper sign applies. In Eqs. (20) and (21), $\mathbf{v}_\alpha \equiv d\mathbf{x}_\alpha/dt|_{t=t_\alpha}$ and $\mathbf{a}_\alpha \equiv d\mathbf{v}_\alpha/dt|_{t=t_\alpha}$ are, respectively, the other charge's velocity and acceleration evaluated at either the retarded or at the advanced lightcone. Notice in Eq. (19) that the electromagnetic sector of the Euler-Lagrange equation involves a semi-sum of the Liénard-Wiechert fields (20) and (21) combined in the Lorentz-force form [16]. Last, in Eqs. (20) and (21) the unit vector from \mathbf{x}_α to $\mathbf{x}_i(t_i)$ is defined by (5). Multiplying (19) by \mathbf{v}_i yields

$$\frac{(m_i + \varepsilon \mathbf{G}_i)}{(1 - \mathbf{v}_i^2)^{3/2}} \mathbf{v}_i \cdot \mathbf{a}_i = \left(\frac{1}{2} e_i \sum_{\alpha=k, j} \mathbf{E}_{\alpha i} \cdot \mathbf{v}_i \right) - \varepsilon \sqrt{1 - \mathbf{v}_i^2} \left(\mathbf{v}_i \cdot \nabla_i \mathbf{G}_i + \gamma_i^2 \mathbf{v}_i^2 \frac{d\mathbf{G}_i}{dt_i} \right), \quad (22)$$

and substituting (22) into the left-hand side of (19) and using (18) yields

$$\left(\frac{m_i + \varepsilon \mathbf{G}_i}{\sqrt{1 - \mathbf{v}_i^2}} \right) \mathbf{a}_i = \frac{1}{2} e_i \sum_{\alpha=k, j} \left(\mathbf{E}_{\alpha i} + \mathbf{v}_i \times \mathbf{B}_{\alpha i} - (\mathbf{v}_i \cdot \mathbf{E}_{\alpha i}) \mathbf{v}_i \right) + \frac{\varepsilon}{2} \sum_{\alpha=k, j} \mathbf{f}_{\alpha i}, \quad (23)$$

where

$$\mathbf{f}_{\alpha i} = \sqrt{1 - \mathbf{v}_i^2} (\nabla_i G_i + \frac{\partial G_i}{\partial t_i} \mathbf{v}_i) \equiv \frac{b_{\alpha i} (\hat{\mathcal{R}}_\alpha \cdot \mathbf{a}_\alpha) \mathbf{u}_{\alpha i}}{(1 \pm \mathbf{n}_\alpha \cdot \mathbf{v}_i)} + c_{\alpha i} \Omega_{\alpha i}^\dagger, \quad (24)$$

$$\mathbf{u}_{\alpha \beta} \equiv (\mathbf{n}_\alpha \pm \mathbf{v}_\beta) \text{ for } \alpha \in (k, j), \beta \in (\alpha, i), \quad (25)$$

$$\Omega_{\alpha i}^\dagger \equiv \left(\frac{1 - \mathbf{v}_\alpha^2}{1 \pm \mathbf{n}_\alpha \cdot \mathbf{v}_\alpha} \right) \mathbf{n}_\alpha \mp (\mathbf{v}_\alpha + \mathbf{v}_i) \text{ for } \alpha \in (k, j), \quad (26)$$

$$b_{\alpha i} \equiv \sqrt{\frac{1 - \mathbf{v}_i^2}{1 - \mathbf{v}_\alpha^2}} \left(\frac{1}{r_{\alpha i} (1 \pm \mathbf{n}_\alpha \cdot \mathbf{v}_\alpha)} \right) \left(\frac{dt_\alpha}{dt_i} \right), \quad (27)$$

$$c_{\alpha i} \equiv \sqrt{\frac{1 - \mathbf{v}_i^2}{1 - \mathbf{v}_\alpha^2}} \left(\frac{e_i \mathbf{n}_\alpha \cdot \mathbf{E}_{\alpha i}}{e_i e_\alpha} \right), \quad (28)$$

$$\hat{\mathcal{R}}_\alpha \equiv \left(\frac{1 - \mathbf{v}_\alpha^2}{1 \pm \mathbf{n}_\alpha \cdot \mathbf{v}_\alpha} \right) \mathbf{n}_\alpha \pm \mathbf{v}_\alpha. \quad (29)$$

Observations: (i) the second term on the right-hand side of (24) is acceleration-independent, (ii) the dagger in Eqs. (24) and (26) indicates that the sign convention is reversed for the second \pm of formula (26), (iii) on the right-hand side of Eq. (27) we have introduced the derivative of time t_α respect to t_i , as obtained by taking a derivative of the lightcone condition (2), i.e.,

$$\frac{dt_\alpha}{dt_i} = \left(\frac{dt_i}{dt_\alpha} \right)^{-1} \equiv \left(\frac{1 \pm \mathbf{n}_\alpha \cdot \mathbf{v}_i}{1 \pm \mathbf{n}_\alpha \cdot \mathbf{v}_\alpha} \right), \quad (30)$$

(iv) the positivity of the right-hand side of (30) ensures that all deviating times are monotonically increasing, (v) Eq. (25) is generalized to be used in several places of the manuscript. The upper sign applies when (α, β) is either (j, j) or (j, i) , while the minus sign applies when (α, β) is either (k, k) or (k, i) , (vi) in Eqs. (24), (26), (27), (28) and (29), the upper sign applies when $\alpha = j$, while the lower sign applies when $\alpha = k$, (vii) the electric field $\mathbf{E}_{\alpha i}$ appearing in Eq. (28) is defined by Eq. (20), (viii) notice that Eq. (22) also follows from Eq. (23), and henceforth equation (23) is called the **equation of motion of particle i**, as derived from partial Lagrangian (14), in which case the advanced index is $\alpha = j$ and the retarded index is $\alpha = k$. The **equation of motion of particle k** is obtained by replacing i with k in Eq. (23) and restricting the summation to the nearest neighbors of index k on the sewing chain of Fig. 1, i.e., $\alpha \in (s, i)$, in which case the most advanced index is $\alpha = i$, (ix) the future and the past lightcones exchange positions upon time-reversal, and in the next section we show that the time-reversible dynamics defines a flow on $C^2(\mathbb{R})$ when $\varepsilon \neq 0$, and (x) notice on the right-hand side of (24) that the far-fields of the ε -sector have non-zero components along \mathbf{n}_j and along the vector $\hat{\mathcal{R}}_\alpha$ defined by (29), i.e.,

$$\mathbf{u}_{\alpha \alpha} \cdot \mathbf{n}_\alpha = (1 \pm \mathbf{n}_\alpha \cdot \mathbf{v}_\alpha) \geq 0, \quad (31)$$

$$\mathbf{u}_{\alpha \alpha} \cdot \hat{\mathcal{R}}_\alpha = (1 \pm \mathbf{n}_\alpha \cdot \mathbf{v}_\alpha) \geq 0, \quad (32)$$

where again $\alpha \in (j, k)$, the upper sign applies when $\alpha = j$, and the lower sign applies when $\alpha = k$.

D. Weierstrass-Erdmann extremum conditions

On breaking points, the Weierstrass-Erdmann extremum conditions must be satisfied instead of the Euler-Lagrange equation. These are the continuity of each partial momentum and of each partial energy **at** the breaking point. The partial momentum derived from the partial Lagrangian (14) is

$$\mathbf{P}_i \equiv \frac{\partial \mathcal{L}_i}{\partial \mathbf{v}_i} = (m_i + \varepsilon \mathbf{G}_i) \gamma_i \mathbf{v}_i + e_i \mathbf{A}_i, \quad (33)$$

where \mathbf{A}_i and \mathbf{G}_i are defined respectively by (16) and (18) and

$$\gamma_\alpha \equiv \frac{1}{\sqrt{1 - \mathbf{v}_\alpha^2}}, \quad (34)$$

for $\alpha \in (i, k)$. The partial energy of the partial Lagrangian (14) is

$$\mathcal{E}_i \equiv \mathbf{v}_i \cdot \frac{\partial \mathcal{L}_i}{\partial \mathbf{v}_i} - \mathcal{L}_i = (m_i + \varepsilon \mathbf{G}_i) \gamma_i + e_i \mathcal{U}_i, \quad (35)$$

where \mathcal{U}_i and \mathbf{G}_i are defined respectively by (17) and (18) and again γ_i is defined by (34). At every breaking point, there is a velocity defined from the left-hand side and a different velocity defined from the right-hand side. The velocity jump must be compensated by the past and future velocity jumps of the other particle in order for (33) and (35) to be continuous at the breaking point.

3. The method of steps

Here we show that the equations of motion (23) can be integrated forward like an ODE when $\varepsilon \neq 0$ and the initial datum belongs to the set of trajectory segments with a full-swing sewing chain in $C^2(\mathbb{R})$, as explained in Fig. 3. The case when $\varepsilon = 0$ is henceforth called electrodynamics and discussed in §7-D. The method of steps illustrated in Fig. 3 and explained in the caption of Fig. 3 uses the most advanced acceleration of each equation of motion as an ODE for the other particle.

A. Reconstruction of the most advanced acceleration

For $\varepsilon = 0$, the left-hand side of (23) contains the acceleration in a linear form inherited from the far-field component of (20), i.e., $\mathbf{n}_\alpha \times ((\mathbf{n}_\alpha + \mathbf{v}_\alpha) \times \mathbf{a}_\alpha)$, which linear form vanishes along the eigendirection

$$\mathbf{a}_\alpha \propto \mathbf{u}_{\alpha\alpha} \equiv (\mathbf{n}_\alpha + \mathbf{v}_\alpha), \quad (36)$$

where the last equality is definition (25) for $\mathbf{u}_{\alpha\alpha}$. The acceleration can be reconstructed using a geometric identity, i.e.,

$$\mathbf{a}_\alpha = \frac{\mathbf{n}_\alpha \cdot \mathbf{a}_\alpha}{(1 + \mathbf{n}_\alpha \cdot \mathbf{v}_\alpha)} (\mathbf{n}_\alpha + \mathbf{v}_\alpha) - \frac{\mathbf{n}_\alpha \times ((\mathbf{n}_\alpha + \mathbf{v}_\alpha) \times \mathbf{a}_\alpha)}{(1 + \mathbf{n}_\alpha \cdot \mathbf{v}_\alpha)}. \quad (37)$$

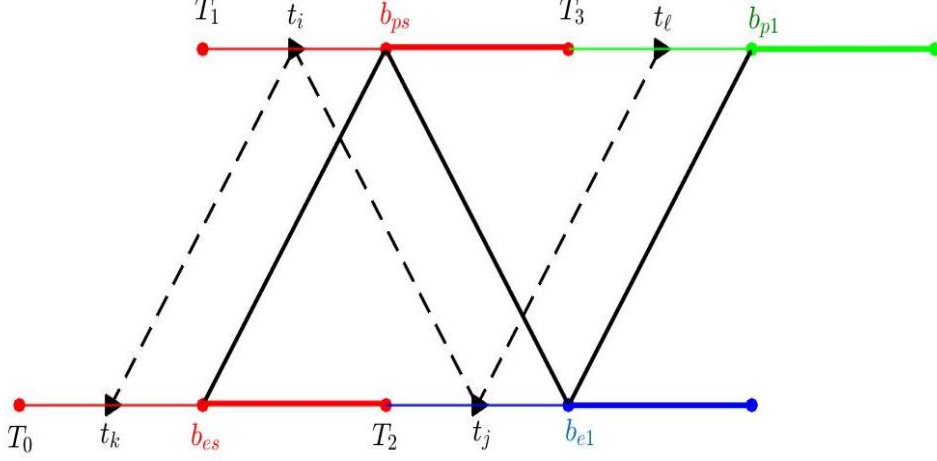


Figure 3: The segments needed for the method of steps are the positions, velocities and accelerations during the time intervals $[T_1, T_3]$ and $[T_0, T_2]$ with respective endpoints in lightcone. The most advanced leg of each equation of motion is used to extend the other particle's trajectory. In order to extend the electronic trajectory using the most advanced electronic acceleration at time t_j , the protonic equation of motion is used with present time t_i running inside the upper red segment, $t_i \in [T_1, T_3]$, to draw the lower blue segment. Simultaneously, the electronic equation of motion is used with present time running from $t_j = T_2$ and past protonic time running from $t_i = T_1$. The electronic acceleration at time t_j runs on the newly created lower blue segment, while the most advanced protonic acceleration produces the upper green extension of the protonic trajectory at time t_ℓ . One step of integration must integrate the electronic equation of motion until t_j reaches the end of the blue segment, when the past protonic time is $t_i = T_3$, thus making the upper green and lower blue segments simultaneously for another full swing of the sewing chain. This is our basic method of steps.

The last term on the right-hand side of (37) is proportional to the acceleration linear-form contained in the near-field of (20), i.e., the $\frac{1}{r_{ji}}$ component. Because of Eq. (21), the right-hand side of (23) is a function of \mathbf{E}_{ji} only. The existence of the null direction (36) prevents the most advanced acceleration \mathbf{a}_j to be reconstructed from the right-hand side of (23). In other words, the value of E_{ji} does not define the coefficient $\mathbf{n}_j \cdot \mathbf{a}_j$ of the first term on the right-hand side of (37). This is the reason we had to perturb electrodynamics in the first place. An identity displaying the rank-deficiency is obtained by comparing definition (29) with a re-arranged version of the scalar product of \mathbf{v}_α with formula (20), yielding

$$\begin{aligned}
\mathbf{n}_\alpha \cdot \mathbf{a}_\alpha &= \hat{\mathcal{R}}_\alpha \cdot \mathbf{a}_\alpha + \frac{\mathbf{v}_\alpha \cdot [\mathbf{n}_\alpha \times (\mathbf{u}_{\alpha\alpha} \times \mathbf{a}_\alpha)]}{(1 + \mathbf{n}_\alpha \cdot \mathbf{v}_\alpha)} \\
&= \hat{\mathcal{R}}_\alpha \cdot \mathbf{a}_\alpha + \frac{\mathbf{v}_\alpha \cdot [(\mathbf{n}_\alpha \cdot \mathbf{u}_{\alpha\alpha})\mathbf{E}_{ji} - (\mathbf{n}_\alpha \cdot \mathbf{E}_{ji})\mathbf{u}_{\alpha\alpha}]}{\zeta_{\alpha i}(\mathbf{n}_\alpha \cdot \mathbf{u}_{\alpha\alpha})^2}, \quad (38)
\end{aligned}$$

where

$$\zeta_{\alpha i} \equiv \frac{e_{\alpha}}{r_{\alpha i}(1 + \mathbf{n}_{\alpha} \cdot \mathbf{v}_{\alpha})^3}. \quad (39)$$

Notice on the numerator of the second equality of (38) that we have subtracted the near-field from \mathbf{E}_{ji} . The reconstruction of \mathbf{a}_{α} with (37) and (38) requires the linear form $\hat{\mathcal{R}}_{\alpha} \cdot \mathbf{a}_{\alpha}$, as provided by the far-field perturbation (24) **plus** the information contained in the electric field (20).

B. ε -strong interaction cures rank deficiency

The equation of motion (23) can be re-arranged with the most advanced acceleration terms on the left-hand side, i.e.,

$$F_{ji}^{e\ell} + \varepsilon b_{ji} \hat{\mathcal{R}}_j \cdot \mathbf{a}_j \left(\frac{\mathbf{u}_{ji}}{\mathbf{n}_j \cdot \mathbf{u}_{ji}} \right) = \Lambda_i^{\text{dat}}, \quad (40)$$

where

$$F_{\alpha i}^{e\ell} \equiv e_i(1 \pm \mathbf{n}_{\alpha} \cdot \mathbf{v}_i) \mathbf{E}_{\alpha i} \mp e_i(\mathbf{v}_i \cdot \mathbf{E}_{\alpha i}) \mathbf{u}_{\alpha i}, \quad (41)$$

$$\Lambda_i^{\text{dat}} \equiv 2(m_i + \varepsilon \mathbf{G}_i) \gamma_i \mathbf{a}_i - F_{ki}^{e\ell} - \varepsilon \Upsilon_i, \quad (42)$$

and

$$\Upsilon_i \equiv c_{ji} \mathbf{\Omega}_{ji}^{\dagger} + c_{ki} \mathbf{\Omega}_{ki}^{\dagger} + \varepsilon b_{ki} \hat{\mathcal{R}}_k \cdot \mathbf{a}_k \left(\frac{\mathbf{u}_{ki}}{\mathbf{n}_k \cdot \mathbf{u}_{ki}} \right). \quad (43)$$

Observations: (i) $\mathbf{E}_{\alpha i}$ is defined by (20) in Eq. (41), (ii) in Eq. (40), the term containing the most advanced acceleration \mathbf{a}_j was passed to the left-hand side while the remaining terms were collected in formula (43) with Υ_i representing **two times** the remaining non-electromagnetic terms of the right-hand side of (23), (iii) the scalar product of the left-hand side of (40) with the killing-vector

$$\mathbb{k}_{\alpha i} \equiv \left(\frac{1 - \mathbf{v}_i^2}{1 \pm \mathbf{n}_{\alpha} \cdot \mathbf{v}_i} \right) \mathbf{n}_{\alpha} \pm \mathbf{v}_i, \quad (44)$$

for $\alpha = j$ vanishes the acceleration term of the electromagnetic sector because $\mathbb{k}_{\alpha i}$ is a left null-vector of the acceleration form $F_{\alpha i}^{e\ell}$, i.e.,

$$F_{ji}^{\circ} \equiv \mathbb{k}_{ji} \cdot F_{ji}^{e\ell} = (1 - \mathbf{v}_i^2)(e_i \mathbf{n}_j \cdot \mathbf{E}_{ji}) = \frac{e_i e_j (1 - \mathbf{v}_i^2)(1 - \mathbf{v}_j^2)}{r_{ji}^2 (1 + \mathbf{n}_j \cdot \mathbf{v}_j)^2}. \quad (45)$$

The acceleration-independent reminder (45) is due to the near-field, (iv) in order to reconstruct the acceleration \mathbf{a}_j using (37) and (38) with $\alpha = j$ we need $\hat{\mathcal{R}}_j \cdot \mathbf{a}_j$, which elusive ingredient is recovered from the scalar product of \mathbb{k}_{ji} with (40) **only** at $O(\varepsilon)$, i.e.,

$$\varepsilon b_{ji} \hat{\mathcal{R}}_j \cdot \mathbf{a}_j = \mathbb{k}_{ji} \cdot \Lambda_i^{\text{dat}} - F_{ji}^{\circ}. \quad (46)$$

In Eq. (46) we have used

$$\mathbb{k}_{ji} \cdot \mathbf{u}_{ji} = \mathbf{n}_j \cdot \mathbf{u}_{ji} = (1 + \mathbf{n}_j \cdot \mathbf{v}_i). \quad (47)$$

Equation (46) at $\varepsilon = 0$ is a constraint on the possible values of Λ_i^{dat} . Otherwise, when $\varepsilon \neq 0$, the right-hand side of (46) involves $\hat{\mathcal{R}}_j \cdot \mathbf{a}_j$ multiplied by a non-zero coefficient, and Λ_i^{dat} is unconstrained. In order to solve for $F_{ji}^{e\ell}$ in terms of the past data, we subtract Eq. (46) multiplied by $\mathbf{u}_{ji}/(\mathbb{k}_{ji} \cdot \mathbf{u}_{ji})$ from Eq. (40) and re-arrange, yielding

$$F_{ji}^{e\ell} = \frac{F_{ji}^o}{(1 + \mathbf{n}_j \cdot \mathbf{v}_i)} \mathbf{u}_{ji} - \frac{\mathbb{k}_{ji} \times (\mathbf{u}_{ji} \times \Lambda_i^{\text{dat}})}{(1 + \mathbf{n}_j \cdot \mathbf{v}_i)}, \quad (48)$$

where again we have used (47) and (v) we can calculate $e_i \mathbf{v}_i \cdot \mathbf{E}_{ji}$ by taking the scalar product of \mathbf{v}_i with the two lines on the right-hand side of (41). After dividing away the scalar product by the non-zero factor $(1 - \mathbf{v}_i^2)$ and substituting the resulting formula for $e_i \mathbf{v}_i \cdot \mathbf{E}_{ji}$ back into (41) we have a formula for \mathbf{E}_{ji} in terms of $F_{ji}^{e\ell}$, i.e.,

$$e_i (\mathbf{n}_j \cdot \mathbf{u}_{ji}) \mathbf{E}_{ji} = \gamma_i^2 \left(F_{ji}^{e\ell} \pm (\mathbf{v}_i \cdot F_{ji}^{e\ell}) \mathbf{n}_j + \mathbf{v}_i \times (\mathbf{v}_i \times F_{ji}^{e\ell}) \right). \quad (49)$$

Notice that because of (48), Eq. (49) defines \mathbf{E}_{ji} in terms of the past data.

C. Differential-delay equation of motion with two delays of neutral type

Numerical integration of differential-delay equations with two delays is a topic of modern interest, e.g., [17, 18]. In order to prepare a numerical study using, for example, the function `ddensd` of MATLAB, we put together the equation of motion of particle j by reconstructing its acceleration with (38), (46) and (49). Solving the first identity of (38) for \mathbf{a}_j we obtain

$$\frac{1}{r_{ji}} \left(\frac{dt_j}{dt_i} \right) \mathbf{a}_j = \frac{1}{r_{ji}} \left(\frac{dt_j}{dt_i} \right) (\hat{\mathcal{R}}_j \cdot \mathbf{a}_j) \left(\frac{\mathbf{u}_{jj}}{\mathbf{n}_j \cdot \mathbf{u}_{jj}} \right) - \frac{1}{e_i e_j} \mathbf{S}_{ji}, \quad (50)$$

where the gyroscopic term \mathbf{S}_{ji} is defined by

$$\mathbf{S}_{ji} \equiv e_i (\mathbf{n}_j \cdot \mathbf{u}_{jj}) (\mathbf{n}_j \cdot \mathbf{u}_{ji}) \left(\mathbf{E}_{ji} - \hat{\mathcal{R}}_j \cdot \mathbf{E}_{ji} \left(\frac{\mathbf{u}_{jj}}{\mathbf{n}_j \cdot \mathbf{u}_{jj}} \right) \right), \quad (51)$$

with \mathbf{E}_{ji} expressed in terms of past data by (48) and (49). In order to express the gyroscopic term as a function of past data, we define the relative angular velocities by

$$\ell_{\alpha\beta} \equiv \mathbf{n}_\alpha \times \mathbf{v}_\beta, \quad (52)$$

and define the nonlinear spin vector by

$$\mathbb{L}_{\mathbf{E}} \equiv e_i (\mathbf{n}_j \cdot \mathbf{u}_{ji}) \mathbf{n}_j \times \mathbf{E}_{ji} = \mathbf{n}_j \times F_{ji}^{e\ell} + \gamma_i^2 (\mathbf{v}_i \cdot F_{ji}^{e\ell}) \ell_{ji}, \quad (53)$$

where ℓ_{ji} is defined by (52). Because of (48), Eq. (53) defines $\mathbb{L}_{\mathbf{E}}$ in terms of past data only. Using (53) to express the gyroscopic term (51) we have

$$\begin{aligned} S_{ji} = & \left((\mathbf{n}_j \cdot \mathbf{u}_{ji}) \ell_{jj}^2 e_i \mathbf{n}_j \cdot \mathbf{E}_{ji} - \mathbf{n}_j \cdot \mathbf{u}_{jj} \ell_j \cdot \mathbb{L}_{\mathbf{E}} \right) \mathbf{n}_j - (\mathbf{n}_j \cdot \mathbf{u}_{jj}) \mathbf{n}_j \times \mathbb{L}_{\mathbf{E}} \\ & + \left(\ell_{jj} \cdot \mathbb{L}_{\mathbf{E}} + (\mathbf{n}_j \cdot \mathbf{u}_{ji}) (\mathbf{n}_{jj} \cdot \mathbf{u}_{jj} - \ell_{jj}^2) e_i \mathbf{n}_j \cdot \mathbf{E}_{ji} \right) \left(\frac{\mathbf{n}_j \times \ell_{jj}}{\mathbf{n}_{jj} \cdot \mathbf{u}_{jj}} \right). \end{aligned} \quad (54)$$

where ℓ_{jj} is defined by (52) and $\mathbb{L}_{\mathbf{E}}$ is defined by (53). In order to display (50) in its explicit singular form, we multiply (50) by ε and use (46) to eliminate $\varepsilon \hat{\mathcal{R}}_j \cdot \mathbf{a}_j$, yielding

$$\frac{\varepsilon}{r_{ji}} \left(\frac{dt_j}{dt_i} \right) \mathbf{a}_j = \left(\frac{dt_j}{dt_i} \right) \left(\frac{\mathbb{k}_{ji} \cdot \Lambda_i^{\text{dat}} - F_{ji}^o}{b_{ji} r_{ji}} \right) \left(\frac{\mathbf{u}_{jj}}{\mathbf{n}_j \cdot \mathbf{u}_{jj}} \right) - \frac{\varepsilon}{e_i e_j} S_{ji}, \quad (55)$$

where F_{ji}^o is defined by (45). Observations: (i) the equation of motion for the most advanced protonic acceleration, \mathbf{a}_ℓ , is obtained from (55) by shifting the indices with the permutation $(kij) \rightarrow (ijl)$, (ii) the gyroscopic term S_{ji} includes a longitudinal term along the direction \mathbf{n}_j with a coefficient that is a nonlinear function of the transverse quantities (53) and (52), (iii) the quantity $\mathbf{n}_j \cdot \mathbf{E}_{ji}$ appearing in the right-hand side of (54) is independent of the most advanced acceleration and (iv) both sides of the equation of motion (55) are **linear** on the accelerations \mathbf{a}_j , \mathbf{a}_i and \mathbf{a}_k .

Theorem 3.1. *Equation (55) with $\varepsilon \neq 0$ defines the most advanced acceleration in $C^2(\mathbb{R})$ when the past data involved in Λ_i^{dat} belong to $C^2(\mathbb{R})$.*

Proof. The proof is the reconstruction of the most advanced acceleration \mathbf{a}_j in $C^2(\mathbb{R})$ using Eq. (55) and past data belonging to $C^2(\mathbb{R})$. An equation of motion for the most advanced protonic acceleration, \mathbf{a}_ℓ , is obtained from (55) by shifting the indices according to the permutation $(kij) \rightarrow (ijl)$. \square

NDDE (55) can start from arbitrary full-swing past data segments in $C^2(\mathbb{R})$. The existence of a semiflow like (55) is already a **stability property**, because the dynamics can propagate and possibly persist in a serrated orbit of $C^2(\mathbb{R})$. Notice that the right-hand side of (55) is independent of the most advanced accelerations \mathbf{a}_j and \mathbf{a}_ℓ . Again, the protonic equation of motion for \mathbf{a}_ℓ is obtained from (55) by shifting the indices $(kij) \rightarrow (ijl)$. This completes the method of steps explained in the caption of Fig. 3. NDDE (55) together with its index-shifted protonic equation for \mathbf{a}_ℓ can be used to build the function **ddensd** of MATLAB.

D. Unfolding Driver's degeneracy

Here we discuss the one-dimensional electromagnetic problems with either repulsive interaction [11, 19] or attractive interaction[8]. After the motion is

restricted to a straight-line by the initial condition segment [8, 11, 19], the Euler-Lagrange equations of electrodynamics turn out to be independent of the most advanced acceleration *and* the far-field interaction vanishes, which is henceforth called Driver's riddle [11]. We start from the one-dimensional version of partial-Lagrangian (14), i.e.,

$$L_i(t_i, \mathbf{x}_i, \mathbf{v}_i) \equiv m_i(1 - \sqrt{1 - \mathbf{v}_i^2}) - \sum_{\alpha=k,j} \frac{1}{2r_{\alpha i}} \left(e_i e_\alpha \mathbf{V}A_{\alpha i}(\mathbf{v}_\alpha, \mathbf{v}_i) + \varepsilon \mathbf{V}G_{\alpha i}(\mathbf{v}_\alpha, \mathbf{v}_i) \right), \quad (56)$$

where $\mathbf{V}A_{\alpha i}(\mathbf{v}_\alpha, \mathbf{v}_i)$ and $\mathbf{V}G_{\alpha i}(\mathbf{v}_\alpha, \mathbf{v}_i)$ are given by

$$\mathbf{V}A_{\alpha i}(\mathbf{v}_\alpha, \mathbf{v}_i) \equiv \frac{(1 - \mathbf{v}_i \cdot \mathbf{v}_\alpha)}{(1 \pm \mathbf{n}_\alpha \cdot \mathbf{v}_\alpha)}, \quad (57)$$

$$\mathbf{V}G_{\alpha i}(\mathbf{v}_\alpha, \mathbf{v}_i) \equiv \frac{\sqrt{1 - \mathbf{v}_i^2} \sqrt{1 - \mathbf{v}_\alpha^2}}{(1 \pm \mathbf{n}_\alpha \cdot \mathbf{v}_\alpha)}. \quad (58)$$

A significant simplification is achieved using *relative* velocity angles $\phi_\alpha \in \mathbb{R}$ for the one-dimensional velocity of each charge, i.e.,

$$\mathbf{v}_\alpha \equiv \tanh \phi_\alpha \mathbf{n}_\alpha \quad (59)$$

and using (59) to express (34) we have

$$\gamma_\alpha = \cosh(\phi_\alpha). \quad (60)$$

We henceforth assume that particle trajectories never collide and the position of each particle falls on its respective side along the light-cone direction $\hat{\mathbf{x}}$, with particle i standing on the right-hand side with a positive coordinate with particle k stands on the left-hand side with a negative coordinate. The former setup leads to $\mathbf{n}_j = \mathbf{n}_k \equiv \hat{\mathbf{x}}$ and $\mathbf{n}_i = \mathbf{n}_s = \mathbf{n}_\ell \equiv -\hat{\mathbf{x}}$. The one-dimensional version of \mathbf{G}_i as defined by (18) is

$$\mathbf{G}_i = \left(\frac{e^{\phi_k}}{2r_{ki}} + \frac{e^{-\phi_j}}{2r_{ji}} \right). \quad (61)$$

In order to describe the details of both the repulsive and the attractive case, we define the relative parameter by

$$\varepsilon_* \equiv -\left(\frac{\varepsilon}{e_\ell e_p} \right). \quad (62)$$

The Euler-Lagrange equation of (56) written in the time-symmetric form is

$$\begin{aligned} \left(m_i + \frac{\varepsilon e^{\phi_k}}{2r_{ki}} + \frac{\varepsilon e^{-\phi_j}}{2r_{ji}} \right) \dot{\phi}_i &= \left(\frac{\varepsilon e^{\phi_k}}{2r_{ki}} \right) \left(\frac{dt_k}{dt_i} \right) \dot{\phi}_k + \left(\frac{\varepsilon e^{-\phi_j}}{2r_{ji}} \right) \left(\frac{dt_j}{dt_i} \right) \dot{\phi}_j \\ &\quad - \frac{e_i e_k e^{2\phi_k}}{2r_{ki}^2 \cosh \phi_i} \left(1 - \varepsilon_* \cosh(\phi_i + \phi_k) \right) \\ &\quad - \frac{e_i e_j e^{-2\phi_j}}{2r_{ji}^2 \cosh \phi_i} \left(1 - \varepsilon_* \cosh(\phi_i + \phi_j) \right), \end{aligned} \quad (63)$$

where (dt_α/dt_i) is defined by (30) and, when expressed by velocity angles for $\alpha \in (k, j)$ standing for a nearest neighbor of i , it becomes

$$\frac{dt_\alpha}{dt_i} = \frac{e^{\mp\phi_\alpha} e^{\mp\phi_i} \cosh \phi_\alpha}{\cosh \phi_i}. \quad (64)$$

Observations: (i) the dot in $\dot{\phi}_\alpha \equiv \frac{d\phi_\alpha}{dt_\alpha}$ indicates derivative respect to time t_α , as always in this manuscript, (ii) the equation for the most advanced protonic acceleration $\dot{\phi}_\ell$ is obtained by shifting the indices $(kij) \rightarrow (ij\ell)$, (iii) Eq. (63) has the acceleration terms proportional to ε/r_{ik} and ε/r_{ij} and when $\varepsilon = 0$ Eq. (63) lacks the most advanced acceleration, giving rise to the riddle found in Refs.[11, 19, 8].

In order to use it in the method of steps, one should solve Eq. (63) for the most advanced derivative, i.e.,

$$\begin{aligned} \varepsilon \left(\frac{e^{-2\phi_j} \cosh \phi_j}{r_{ji}} \right) \dot{\phi}_j &= \left(2m_i + \frac{\varepsilon e^{\phi_k}}{r_{ki}} + \frac{\varepsilon e^{-\phi_j}}{r_{ji}} \right) \cosh \phi_i \dot{\phi}_i \\ &\quad - \varepsilon \left(\frac{e^{2\phi_k} \cosh \phi_k}{r_{ki}} \right) \dot{\phi}_k \\ &\quad + \frac{e_i e_j e^{-2\phi_j}}{r_{ji}^2} \left(1 - \varepsilon_* \cosh(\phi_j + \phi_i) \right) \\ &\quad + \frac{e_i e_k e^{2\phi_k}}{r_{ki}^2} \left(1 - \varepsilon_* \cosh(\phi_i + \phi_k) \right). \end{aligned} \quad (65)$$

As with (63), the equation for $\dot{\phi}_\ell$ corresponding to (65) is obtained by shifting the indices $(kij) \rightarrow (ij\ell)$. For $\varepsilon_* > 0$, the last two lines of (65) vanish identically if the angle of relative approximation reaches the (singular) value

$$\cosh(\phi_e + \phi_p) = \frac{1}{\varepsilon_*} \equiv \cosh 2\phi_\varepsilon, \quad (66)$$

which brings us to the phase-locked segments.

Theorem 3.2. *For $\varepsilon_* > 0$, the method of steps for (65) has a one-parameter family of fixed segments with constant velocities $\dot{\phi}_e(t_e) = \dot{\phi}_e$ and $\dot{\phi}_p(t_p) = \dot{\phi}_p$ such that,*

$$\dot{\phi}_e(t_e) = \dot{\phi}_p(t_p) = 0, \quad (67)$$

$$\phi_e + \phi_p = \pm 2\phi_\varepsilon, \quad (68)$$

for $t_e \in [T_0, T_2]$ and $t_p \in [T_1, T_2]$, as illustrated by the red segments of Fig. 3.

Proof. The proof is by inspection that (65) calculates $\dot{\phi}_e(t_e) = 0$ for the whole blue segment of Fig. 3, and likewise for the protonic green segment of Fig. 3. \square

The motion can continue to satisfy (67) indefinitely. It is further possible to introduce velocity discontinuities in the initial segment. Fig. 3 illustrates the case

of one discontinuity at mid-segment, after which times velocities jump to another pair of constant velocities. Sub-segments $[T_1, b_{ps}]$ and $[T_0, b_{es}]$ are drawn with thinner red lines while sub-segments $[b_{ps}, T_3]$ and $[b_{es}, T_2]$ are drawn with ticker lines in Fig. 3. **If** one could calibrate the discontinuities such that both velocity pairs satisfy some branch of (67) and (68), the orbit will continue with **piecewise constant** velocities for the whole blue and green segments, as found inspecting Fig. 3. Such novel particle of ε -**VE** would have vanishing far-fields because it is a motion with vanishing accelerations. The charges are kept bounded simply by exchanging photonic kicks at breaking points, as discusses in §7-D below. It is beyond the present work to investigate if and for which magnitudes such motions are possible, and if such orbits are stable or not. A few cases of the energetic conditions for velocity discontinuities are studied below.

E. Domains of initial histories

This section is designed to guide future numerical experiments. The most advanced accelerations, \mathbf{a}_j and \mathbf{a}_ℓ , given respectively by (50) and its index-shifted formula, are continuous functions that can be integrated by the method of steps of Fig. 3. For straight-line obits, the equations of motion reduce to Eqs. (65) and its index-shifted formula. Integration must start from sufficiently long orbital segments that include **two** flights of the sewing chain, as illustrated in Fig. 3 and henceforth called **full-swing histories**. Moreover, in order to have a unique extension, we need a subset of $C^2(\mathbb{R})$ where the accelerations are Lipschitz continuous. An obvious non-empty initial-history set to start from when $\varepsilon = 0$ is the set of full-swing segments of circular orbits[22, 14], because circular orbits are globally defined. As noticed in Ref. [9], circular orbits still exist for $\varepsilon \neq 0$ because time-reversal exchanges \mathbf{v} by $-\mathbf{v}$ in Eq. (23), which should be unstable like the $\varepsilon = 0$ circular orbits [14]. If $\varepsilon \neq 0$, the method of steps of Fig. 3 acts as a **semiflow** on the set of full-swing segments of ε -circular orbits: for every $\tau \in \mathbb{R}^+$ and for every full-swing element $\phi_{FS} \in C^2(\mathbb{R})$ with $t_p \in [T_1, T_3]$ and $t_e \in [T_0, T_2]$, the method of steps takes ϕ_{FS} to (another) full-swing element, i.e., $\psi_\tau : (\tau, \phi) \rightarrow C^2(\mathbb{R})$. The function ψ_τ has the semigroup property that $\psi_0 = I$ and $\psi_{\tau_1} \circ \psi_{\tau_2} = \psi_{\tau_1 + \tau_2}$. Moreover, restricted to the set of full-swing circular segments we can use the method of steps for $\tau \in \mathbb{R}$, i.e., ψ_τ has the **group** property and it defines a **flow**. In the following we attempt to construct larger initial-history sets where the method of steps would operate either as a semiflow or as a flow.

Inspecting Eq. (50) we find that \mathbf{a}_j is bounded if $r_{ji} \mathbf{n}_j \cdot \mathbf{E}_{ji}$ is bounded. Analogously, using the index-shifted (50) we find that \mathbf{a}_ℓ is bounded whenever $r_{\ell j} \mathbf{n}_\ell \cdot \mathbf{E}_{\ell j}$ is bounded. Inside the Peano domain (12), our Eq. (50) is an ODE with a bounded right-hand side. Using Lemma 2.1 and Eq. (50) we also find that, whenever the orbit belongs to the Peano domain (12), one can define a new independent variable $\xi_j \in \mathbb{R}$ for the \mathbf{a}_j equation of motion and a new independent

variable $\xi_\ell \in \mathbb{R}$ for the \mathbf{a}_ℓ equation, i.e.,

$$\xi_\ell \equiv \int \frac{dt_\ell}{r_{\ell j}(1 - \mathbf{v}_\ell^2)} \quad \text{and} \quad \xi_j \equiv \int \frac{dt_j}{r_{ji}(1 - \mathbf{v}_j^2)}, \quad (69)$$

If the minimizer orbit belongs to (12), we can integrate the method of steps until a full-swing. Notice that (50) with $\varepsilon \neq 0$ is an accomplishment in itself above the Coulomb problem, since the integration of (50) is simpler than the gravitational problem, as follows: (i) the singularity in the $\varepsilon \neq 0$ case is proportional to $1/r_{ji}$ (versus $1/r_{ji}^2$ for the gravitational problem), and (ii) a change of the integration variable like (69) would not work for the gravitational problem. In fact, a similar coordinate transformation is just one of the many transformations involved in the Levi-Civita regularization[24].

A Lipschitz set of initial segments must avoid a head-on collision **and** prevent superluminal orbits. The Lipschitz condition [20] places a bound on the right-hand side of (65), limiting the ϕ_α by $\max\{|\phi_\alpha|\} < B_\alpha(\min\{r_{ep}\})$. Collisions act as Lipschitz moderators that keep the delay bounded away from zero by bouncing the trajectories. A way to cure arbitrary full-swing segments is to introduce collisions-at-a-distance as perturbations designed to avoid both the physical collision[20] and a luminal velocity by enforcing

$$0 < \delta_1 < \min(r_{ji}(1 - \mathbf{v}_j^2), r_{\ell j}(1 - \mathbf{v}_\ell^2)). \quad (70)$$

Because of Lemma 2.1, if the orbit satisfies (70), the general equation of motion (50) has finite denominators defining the terms for $r_{ji} \mathbf{n}_j \cdot \mathbf{E}_{ji}$ and $r_{\ell i} \mathbf{n}_\ell \cdot \mathbf{E}_{\ell i}$. As the integration marches forward, whenever the orbit violates (70), we can halt the integration and modify the history by introducing a collision-at-a-distance with a convenient velocity-discontinuity designed to enforce (70). Integration must be re-calculated with the last two flights of the modified history, while the remaining segments should either be discarded or used in a perturbation theory analogous to the one described in Ref. [25]. The best type of collision-at-a-distance to use in a perturbation theory is the mutual-recoil collision-at-a-distance, as described in the outer-cone Lemma 7.1 of §7-B.

4. Forward continuation of velocity discontinuities

A. *A priori continuation based on the continuity of the partial momenta*

For initial data belonging to $\hat{C}^2(\mathbb{R})$, the method of steps proceeds piecewise; Fig. 3 illustrates a generic breaking point defined by a pair of velocity discontinuities in lightcone at times ($t_i = b_{es}, t_k = b_{ps}$) respectively on the electronic and protonic trajectories. At the breaking point we must halt the forward integration to try and see **if** the four continuity conditions (33) and (35) are satisfied. We start by showing that the three continuity conditions of Eq. (33) are sufficient to

propagate the velocity of each particle across the discontinuity. Notice that (33) involves **three** velocity vectors, i.e., \mathbf{v}_i , \mathbf{v}_k and \mathbf{v}_j , which allows one to consider \mathbf{v}_i and \mathbf{v}_k as independent variables and solve (33) for the most advanced velocity \mathbf{v}_j . The former inversion can be performed only inside proper domains, as we explain in the next three Lemmas.

The continuous partial momentum (33) splits in a term containing the most advanced velocity \mathbf{v}_j and a local part containing only \mathbf{v}_i and \mathbf{v}_k , i.e.,

$$\mathbf{P}_i \equiv m_i \gamma_i \mathbf{v}_i - \mathbf{a}_{ki}(\mathbf{v}_k, \mathbf{v}_i) - \mathbf{a}_{ji}(\mathbf{v}_j, \mathbf{v}_i), \quad (71)$$

where

$$\mathbf{a}_{ji}(\mathbf{v}_j) \equiv \frac{-1}{2r_{ji}(1 + \mathbf{n}_j \cdot \mathbf{v}_j)} (e_i e_j \mathbf{v}_j + \varepsilon \gamma_i \sqrt{1 - \mathbf{v}_j^2} \mathbf{v}_i), \quad (72)$$

$$\mathbf{a}_{ki}(\mathbf{v}_k) \equiv \frac{-1}{2r_{ki}(1 - \mathbf{n}_k \cdot \mathbf{v}_k)} (e_i e_k \mathbf{v}_k + \varepsilon \gamma_i \sqrt{1 - \mathbf{v}_k^2} \mathbf{v}_i). \quad (73)$$

At the breaking point for \mathbf{v}_i , the discontinuity of the future velocity \mathbf{v}_j makes the quantity

$$\mathbf{a}_{ji} \equiv \left(m_i \gamma_i \mathbf{v}_i - \mathbf{P}_i \right) - \mathbf{a}_{ki}, \quad (74)$$

to be discontinuous in order to compensate for the discontinuities of \mathbf{v}_i and \mathbf{v}_k . Equation (74) defines \mathbf{a}_{ji} as a function of \mathbf{a}_{ki} on both sides of the breaking point. In the following we invert definitions (72) and (73) in order to express either \mathbf{v}_j or \mathbf{v}_k as a function of $\mathbf{a}_{\alpha i}$, ε , the present velocity, and either the future or the past velocity, e.g., $\mathbf{v}_j = \vec{\rho}(\mathbf{a}_{ji}, \varepsilon, \mathbf{n}_j, \mathbf{v}_i, \mathbf{v}_k)$. The generalized expression for \mathbf{v}_α is used in many places of the manuscript, i.e.,

$$\mathbf{v}_\alpha \equiv \vec{\rho}(\mathbf{a}_{\alpha i}) + \varepsilon_* \gamma_i \sqrt{1 - \mathbf{v}_\alpha^2} \vec{q}(\mathbf{a}_{\alpha i}, \mathbf{n}_j, \mathbf{v}_i), \quad (75)$$

where ε_* is defined by (62), the functions $\vec{\rho}(\mathbf{a}_{\alpha i}, \mathbf{n}_\alpha, r_{\alpha i}): \mathbb{R}^3 \times \mathbb{R}^3 \times \mathbb{R} \rightarrow \mathbb{R}^3$ and $\vec{q}(\mathbf{a}_{\alpha i}, \mathbf{n}_\alpha, \mathbf{v}_i): \mathbb{R}^3 \times \mathbb{R}^3 \times \mathbb{R}^3 \rightarrow \mathbb{R}^3$ are defined by

$$\vec{\rho}(\mathbf{a}_{\alpha i}, \mathbf{n}_\alpha, r_{\alpha i}) \equiv \frac{2r_{\alpha i} \mathbf{a}_{\alpha i}}{(-e_i e_\alpha \mp 2r_{\alpha i} \mathbf{n}_j \cdot \mathbf{a}_{\alpha i})} = \frac{\mathbf{a}_{\alpha i}}{\left(\frac{-e_i e_\alpha}{2r_{\alpha i}} \mp \mathbf{n}_\alpha \cdot \mathbf{a}_{\alpha i} \right)}, \quad (76)$$

$$\vec{q}(\mathbf{a}_{\alpha i}, \mathbf{n}_\alpha, \mathbf{v}_i) \equiv \mathbf{v}_i \pm (\mathbf{n}_\alpha \cdot \mathbf{v}_i) \vec{\rho}(\mathbf{a}_{\alpha i}), \quad (77)$$

and γ_i is defined by (34). Observations: (i) for economy of notation, we henceforth abbreviate the list of arguments of (76) and (77), keeping only the first argument, e.g., $\vec{\rho}(\mathbf{a}_{\alpha i})$, (ii) the plus sign in every definition below (76) holds when $\alpha = j$, while the minus sign holds when $\alpha = k$, (iii) because the functional (8) is time-reversible, (75) is invariant under a time-reversal operation on the indices if every \pm sign is exchanged, e.g, $(kij) \rightarrow (iks)$. Eq. (75) is also invariant in form under a forward shift of indices, $(kij) \rightarrow (ijl)$.

Lemma 4.1. *Equation (75) with $\varepsilon_* = 0$ defines a **unique** electronic velocity \mathbf{v}_α for each $\mathbf{a}_{ji} \in \mathbb{R}^3$ inside a paraboloid of revolution domain in \mathbb{R}^3 .*

Proof. Squaring (75) for a subluminal orbit when $\varepsilon_* = 0$ yields

$$1 - \mathbf{v}_\alpha^2 = 1 - \|\vec{\rho}(\mathbf{a}_{\alpha i})\|^2 \geq 0. \quad (78)$$

We choose an orthogonal Cartesian system with the $\hat{\mathbf{y}}$ axis along the \mathbf{n}_α direction to evaluate the inequality on the right-hand side (78), finding that $a_y \equiv \pm \mathbf{n}_\alpha \cdot \mathbf{a}_{\alpha i}$ is defined from the subluminal condition $\|\rho_a(\mathbf{a}_{\alpha i})\|^2 < 1$ as

$$a_y \leq \frac{1}{4r_{ij}} - r_{\alpha i}(a_x^2 + a_z^2). \quad (79)$$

Condition (79) defines the interior of a paraboloid of revolution for $\mathbf{a}_{\alpha i} \in \mathbb{R}^3$. \square

Otherwise, when $\varepsilon_* \in \mathbb{R}$, the squared modulus of (75) yields a quadratic equation for $\sqrt{1 - \mathbf{v}_\alpha^2}$, namely

$$(1 - \mathbf{v}_\alpha^2) + 2\mathbf{B}\sqrt{1 - \mathbf{v}_\alpha^2} - \mathbf{C} = 0, \quad (80)$$

where

$$\mathbf{B}(\mathbf{a}_{ji}) \equiv \frac{\varepsilon_* \gamma_i \vec{q}(\mathbf{a}_{\alpha i}) \cdot \vec{\rho}(\mathbf{a}_{\alpha i})}{(1 + \varepsilon_*^2 \gamma_i^2 \|\vec{q}(\mathbf{a}_{\alpha i})\|^2)}, \quad (81)$$

$$\mathbf{C}(\mathbf{a}_{ji}) \equiv \frac{1 - \|\vec{\rho}(\mathbf{a}_{\alpha i})\|^2}{(1 + \varepsilon_*^2 \gamma_i^2 \|\vec{q}(\mathbf{a}_{\alpha i})\|^2)}. \quad (82)$$

The roots of (80) behave as follows: (i) the minus root $(1 - \mathbf{v}_j^2) = -\mathbf{B} - \sqrt{\mathbf{B}^2 + \mathbf{C}}$ never belongs to $[0, 1)$ and (ii) whenever $\mathbf{B} > 0$ and $0 < \mathbf{C} < 1$, the unique root inside $[0, 1)$ is the plus root $(1 - \mathbf{v}_j^2) = -\mathbf{B} + \sqrt{\mathbf{B}^2 + \mathbf{C}}$ with $\mathbf{a}_{ji} \in \mathbb{R}^3$ is inside the paraboloid of Lemma 4.1. The domain where the unique (physical) root $(1 - \mathbf{v}_j^2) = -\mathbf{B} + \sqrt{\mathbf{B}^2 + \mathbf{C}}$ belongs to $[0, 1)$ extends beyond the paraboloid of Lemma 4.1 when $\varepsilon_* \neq 0$ and $-\mathbf{B}^2 < \mathbf{C} \leq 0$, as follows:

Lemma 4.2. *Equation (75) with $\varepsilon_* \neq 0$ defines a **unique** electronic velocity \mathbf{v}_α for each $\mathbf{a}_{\alpha i} \in \mathbb{R}^3$ belonging to the interior of an asymmetric paraboloid domain.*

Proof. As mentioned in item (i) below Eq. (82), the minus root is impossible and the only possible root is given by Bhaskara's formula with the **plus** sign, item (ii) below Eq. (82). The condition for the root to be in $[0, 1)$ is $0 < -\mathbf{B} + \sqrt{\mathbf{B}^2 + \mathbf{C}} < 1$. The upper bound yields the trivial identity $0 < \|\vec{\rho} + \varepsilon_* \gamma_i \vec{q}\|^2$ by use of (81) and (82), while the lower bound yields

$$\rho^2 < 1 + \varepsilon_*^2 \gamma_i^2 q^2 + \varepsilon_*^2 \gamma_i^2 \left((\vec{q} \cdot \vec{\rho})^2 - \rho^2 q^2 \right), \quad (83)$$

thus extending condition (78) of Lemma 4.1. Using (77) to re-arrange (83) yields

$$\rho^2 < 1 + \frac{\varepsilon_*^2 \gamma_i^2 (\mathbf{n}_j \cdot \mathbf{v}_i + \vec{\rho} \cdot \mathbf{v}_i)^2}{1 + \frac{\varepsilon_*^2 \gamma_i^2 \|\ell_{\alpha i}\|^2}{21}}, \quad (84)$$

where $\ell_{\alpha i}$ is defined by Eq. (52). Without loss of generality we take the velocity vector \mathbf{v}_i in a plane xy with the $\hat{\mathbf{y}}$ axis defined along the \mathbf{n}_j direction, i.e.,

$$\mathbf{v}_i \equiv \|\mathbf{v}_i\|(\cos(\vartheta_i)\hat{\mathbf{x}} + \sin(\vartheta_i)\hat{\mathbf{y}}). \quad (85)$$

Substituting (76) and (85) into (84) yields

$$a_y \leq \left(\frac{1 + \varepsilon_*^2 \gamma_i^2 \mathbf{v}_i^2}{4r_{ij}} \right) - r_{ij} a_z^2 - r_{ij} \frac{\left(a_x - \frac{\varepsilon_*^2 \gamma_i^2 \mathbf{v}_i^2 \sin \vartheta_i}{4r_{ij}} \right)^2}{(1 + \varepsilon_*^2 \gamma_i^2 \mathbf{v}_i^2 \cos^2 \vartheta_i)}, \quad (86)$$

which is the interior of an asymmetric paraboloid in the space $a_{\alpha i} \in \mathbb{R}^3$. Notice that (86) reduces to (79) when $\varepsilon_* = 0$, which is the case of Lemma 4.1. \square

The protonic velocity at point ℓ in the sewing-chain of Fig. 1 is obtained from (86) by shifting the indices by one position forward along the sewing chain (o, s, k, i, j, ℓ) , as illustrated in Fig. 2. Condition (86) and the analogous condition for the protonic velocity yield an a priori (tentative) forward continuation of the sewing chain, before ever testing **if** the Weierstrass-Erdmann partial energy (35) is continuous for either particle. Equation (75) of Lemma 4.2 defines the most advanced velocity of either particle for $\alpha \in (j, \ell)$. In the following we use the function $\theta_{\alpha i} : \mathbf{v}_\alpha \in \mathbb{R}^3 \rightarrow \mathbb{R}$ defined from the electronic velocity at sites $\alpha \in (k, j)$, which are either the past lightcone or the future lightcone of point i , i.e.,

$$\theta_{\alpha i} \equiv \frac{\sqrt{1 - \mathbf{v}_\alpha^2}}{1 \pm \mathbf{n}_\alpha \cdot \mathbf{v}_\alpha}. \quad (87)$$

The quantity $\theta_{\alpha i}$ defined by (87) can be expressed in terms of \mathbf{v}_i by the **outsider** Lemma explained next.

Lemma 4.3. *Let $\alpha \in (j, k)$ be the past and the future neighbors of index i on a sewing chain. We have*

$$\frac{\varepsilon \gamma_i \theta_{\alpha i}}{2r_{\alpha i}} = \frac{\varepsilon_*^2 \gamma_i^2}{(1 + \varepsilon_*^2 \gamma_i^2 \|\ell_{\alpha i}\|^2)} \left(\pm \frac{e_\alpha e_i \mathbf{n}_\alpha \cdot \mathbf{v}_i}{2r_{\alpha i}} - \ell_{\alpha i} \cdot (\mathbf{n}_\alpha \times a_{\alpha i}) \right), \quad (88)$$

where $\theta_{\alpha i}$ is defined by (87), $\ell_{\alpha i}$ is defined by (52), ε_* is defined by (62), the plus sign goes with the future index $\alpha = j$, the minus sign goes with the past index $\alpha = k$, and $a_{\alpha i}$ is expressed in terms of \mathbf{v}_i and \mathbf{v}_k either by Eq.(74) when $\alpha = j$ or by its time-reversed version when $\alpha = k$.

Proof. Substituting formula (75) for the unique velocity of Lemma (4.1) into definition (87) we obtain

$$\theta_{\alpha i} = \frac{-\varepsilon_* \gamma_i}{(1 + \varepsilon_*^2 \gamma_i^2 \|\ell_{\alpha i}\|^2)} \frac{\mathbf{v}_i \cdot (\vec{\rho} \pm \mathbf{n}_\alpha)}{(1 \pm \mathbf{n}_\alpha \cdot \vec{\rho})}, \quad (89)$$

expressed in terms of the vector function $\vec{\rho}$. Using the last term of Eq.(76) to eliminate ρ in terms of $a_{\alpha i}$ brings out formula (88). \square

Observations: (i) the elimination of a nearest neighbor leaves a second order reminder, as seen by the ε_*^2 in formula (88) and (ii) **assuming** that the given discontinuities are consistent with Lemma 4.2, we can determine \mathbf{v}_j and \mathbf{v}_ℓ uniquely on the right-hand side of times t_ℓ and t_j using Eq. (75). Otherwise the initial segment predicts **inconsistent** superluminal velocities and can not be continued any further, and (iii) having found \mathbf{v}_j and \mathbf{v}_ℓ on the right-hand side, we still have to see if the jump satisfies the energetic constraints (35) in order to have a minimizer of the action functional (8).

B. Boundary layer of small denominators

As explained in §4-A, Lemma 4.2 is the result of using (33) to continue the sewing chain. The former *tentative* sewing chain still has to satisfy one last Weierstrass-Erdmann condition for each particle, i.e., the energetic constraints (35). In order to enforce (35) we split formula (17) into a continuous part plus a jumping part, i.e.,

$$e_i \mathcal{U}_i = \left(\frac{e_i e_k}{2r_{ki}} + \frac{e_i e_j}{2r_{ji}} \right) + \left(\frac{e_i e_k \mathbf{n}_k \cdot \mathbf{v}_k}{2r_{ki}(1 - \mathbf{n}_k \cdot \mathbf{v}_k)} - \frac{e_i e_j \mathbf{n}_j \cdot \mathbf{v}_j}{2r_{ji}(1 + \mathbf{n}_j \cdot \mathbf{v}_j)} \right), \quad (90)$$

which is to be compared to the scalar product $\mathbf{n}_j \cdot \mathbf{P}_i$, i.e.,

$$\mathbf{n}_j \cdot \mathbf{P}_i = \left(\frac{m_i + \varepsilon \mathbf{G}_i}{\sqrt{1 - \mathbf{v}_i^2}} \right) \mathbf{n}_j \cdot \mathbf{v}_i + \left(\frac{e_i e_k \mathbf{n}_j \cdot \mathbf{v}_k}{2r_{ki}(1 - \mathbf{n}_k \cdot \mathbf{v}_k)} + \frac{e_i e_j \mathbf{n}_j \cdot \mathbf{v}_j}{2r_{ji}(1 + \mathbf{n}_j \cdot \mathbf{v}_j)} \right). \quad (91)$$

Adding (90) to (91) to calculate the partial energy \mathcal{E}_i of (35), defining the **continuous** function

$$\bar{u}_i \equiv \left(\frac{e_i e_k}{2r_{ki}} + \frac{e_i e_j}{2r_{ji}} \right), \quad (92)$$

and using (33) and (35) to eliminate the most advanced velocity \mathbf{v}_j from \mathbf{P}_i and \mathcal{E}_i yields

$$\begin{aligned} \mathbb{C}_i \equiv \mathcal{E}_i + \mathbf{n}_j \cdot \mathbf{P}_i - \bar{u}_i &= \left(\frac{1 + \mathbf{n}_j \cdot \mathbf{v}_i}{\sqrt{1 - \mathbf{v}_i^2}} \right) m_i + \frac{e_i e_k (\mathbf{n}_j + \mathbf{n}_k) \cdot \mathbf{v}_k}{2r_{ki}(1 - \mathbf{n}_k \cdot \mathbf{v}_k)} \\ &\quad + \frac{\varepsilon \gamma_i (1 + \mathbf{n}_j \cdot \mathbf{v}_i) \theta_{ki}}{2r_{ki}} + \frac{\varepsilon \gamma_i (1 + \mathbf{n}_j \cdot \mathbf{v}_i) \theta_{ji}}{2r_{ji}}. \end{aligned} \quad (93)$$

The corresponding energetic condition using the backward shifted formulas (33) and (35) for \mathbf{P}_k and \mathcal{E}_k to eliminate the most retarded velocity \mathbf{v}_s is

$$\begin{aligned} \mathbb{C}_k \equiv \mathcal{E}_k - \mathbf{n}_s \cdot \mathbf{P}_k - \bar{u}_k &= \left(\frac{1 - \mathbf{n}_s \cdot \mathbf{v}_k}{\sqrt{1 - \mathbf{v}_k^2}} \right) m_k - \frac{e_i e_k (\mathbf{n}_s + \mathbf{n}_i) \cdot \mathbf{v}_i}{2r_{ki}(1 + \mathbf{n}_i \cdot \mathbf{v}_i)} \\ &\quad + \frac{\varepsilon \gamma_k (1 - \mathbf{n}_s \cdot \mathbf{v}_k) \theta_{ik}}{2r_{ik}} + \frac{\varepsilon \gamma_k (1 - \mathbf{n}_s \cdot \mathbf{v}_k) \theta_{sk}}{2r_{ks}}. \end{aligned} \quad (94)$$

Observations: (i) the right-hand sides of (93) and (94) are continuous functions of the velocities and define two large-velocity segments on each side of the breaking

point, henceforth the **boundary layer**, and (ii) If $\varepsilon = 0$, Eqs. (93) and (94) are an overdetermination imposed on the velocity pair $(\mathbf{v}_i(t_i = b_{ps}), \mathbf{v}_k(t_k = b_{es}))$, which should be used to test the red segment of Fig. 3 for consistency, and (iii) when $\varepsilon \neq 0$, Eqs. (93) and (94) include **two** inequivalent ε -dependent terms; the first term on the second line of the right-hand sides of either (93) or (94) is a coupling to the $(\mathbf{v}_i, \mathbf{v}_k)$ pair, while the last term of either line introduces couplings to either \mathbf{v}_s or \mathbf{v}_j nearest-neighbor velocities, and need to be eliminated using the outsider Lemma 4.3. As explained in 4.3, the former yields an $O(\varepsilon^2)$ perturbation when expressed back in terms of the $(\mathbf{v}_i, \mathbf{v}_k)$ pair.

5. Straight line collisions-at-a-distance

The velocities must be sufficiently large in (93) and (94) to allow a velocity discontinuity. Here we study the simplest descent to the breaking point, henceforth a straight-line collision-at-a-distance. The velocities before the collision are the natural parameters of the collision, and the one-parameter Lorentz group splits the two-parameter set into boost classes, as discussed in §7-A. For use in the numerical perturbation theory proposed next, an important outcome of the collision is **if** the velocity of relative approximation changes sign or not. We classify two types of collision; (i) **mutual recoil**, when both initially opposite velocities change sign and thus the velocity of relative approximation changes sign, and (ii) **sticky collision**, when both initial velocities were pointed to the same direction and *after* the collision **both** velocities flip sign, in which case the relative approximation might either change sign or not. Inside this section only we shall use the *absolute* velocity angles defining the velocity along $\hat{\mathbf{x}}$ instead of the velocities along the direction $\hat{\mathbf{n}}_\alpha$ defined in (59), i.e.,

$$\mathbf{v}_\alpha \equiv v_\alpha \hat{\mathbf{x}} \equiv \tanh \varphi_\alpha \hat{\mathbf{x}}. \quad (95)$$

Using the setup defined below (60), where $\mathbf{n}_e = \hat{\mathbf{x}}$ and $\mathbf{n}_p = -\hat{\mathbf{x}}$, the absolute angles are expressed in terms of the relative angles (59) by $(\varphi_e, \varphi_p) = (\phi_e, -\phi_p)$. We adopted (95) in order to make the formulas in this section look more symmetric. The velocity of relative approximation in lightcone is

$$\frac{dr_{ki}}{dt_i} = \frac{d(t_i - t_k)}{dt_i} = 1 - \frac{dt_k}{dt_i} = \frac{v_i - v_k}{1 - v_k}, \quad (96)$$

where we have used (30). Using the details below (59) to evaluate Eqs. (93) and (94) in a neighborhood of a one-dimensional collision-at-a-distance we have

$$\begin{aligned} \mathbb{C}_i \equiv \mathcal{E}_i + \mathbf{n}_j \cdot \mathbf{P}_i - \bar{u}_i &= \left(\frac{1 + v_i}{\sqrt{1 - v_i^2}} \right) m_i + \frac{e_i e_k v_k (1 + v_k)}{2r_{ki} (1 - v_k^2)} \\ &+ \frac{\varepsilon}{2r_{ki}} \left(\frac{1 + v_i}{\sqrt{1 - v_i^2}} \right) \left(\frac{1 + v_k}{\sqrt{1 - v_k^2}} \right) \\ &+ \frac{e_i e_k \varepsilon_x^2 (1 + v_i) v_i}{2r_{ji} (1 - v_i^2)}, \end{aligned} \quad (97)$$

where the last $O(\varepsilon^2)$ term was evaluated using Lemma 4.3. In order to express the formulas with an economy of parameters, we henceforth define *scaled* masses

$$M_\alpha \equiv r_{ki} m_\alpha; \quad \alpha \in (i, k). \quad (98)$$

Substituting the hyperbolic velocity-angles (59) into (97) and the analogous version of (94), and disregarding the $O(\varepsilon^2)$ term yields

$$\lambda_i(\varphi_i, \varphi_k) \equiv r_{ki} \mathbb{C}_i + \frac{e_i e_k}{2} = M_i e^{\varphi_i} + \frac{e_i e_k e^{2\varphi_k}}{2} + \frac{\varepsilon e^{\varphi_i} e^{\varphi_k}}{2}, \quad (99)$$

$$\lambda_k(\varphi_i, \varphi_k) \equiv r_{ki} \mathbb{C}_k + \frac{e_i e_k}{2} = M_k e^{\varphi_k} + \frac{e_i e_k e^{2\varphi_i}}{2} + \frac{\varepsilon e^{\varphi_i} e^{\varphi_k}}{2}, \quad (100)$$

a great simplification that preserves the continuity of the left-hand sides of (97) and its electronic counterpart. Elimination of e^{φ_i} from (99) and substitution into (100) yields an algebraic equation of the fourth degree with coefficients depending on the constants $(M_i, M_k, \lambda_i, \lambda_k, e_i e_k, \varepsilon)$. In order to have a discontinuity, the quartic polynomial must have at least **two** positive roots $e^{\varphi_k} \in \mathbb{R}_+$. The collisions-at-a-distance are not all equivalent by the Lorentz group, and in the following we analyze only the most interesting ones. Some surprises are discovered inspecting (99) and (100). In a nutshell, electrodynamics ($\varepsilon = 0$) can have mutual recoils only for the electron-electron case. On the other hand, for the attractive case, only sticky collisions are possible, which distinguishes purely electromagnetic electron-electron collisions-at-a-distance from purely electromagnetic electron-proton collisions-at-a-distance.

Lemma 5.1. *The **collision-at-a-distance** $(\varphi_i, \varphi_k) \rightarrow (-\varphi_i, -\varphi_k)$ when $\varepsilon = 0$ is a **mutual recoil** for the electron-electron collision, $e_i e_k = 1$, and a **sticky collision** for the electron-proton collision, $e_i e_k = -1$.*

Proof. Because the left-hand side of (99) is continuous, at the breaking point along trajectory i we have $\lambda_i(\varphi_i, \varphi_k) - \lambda_i(-\varphi_i, -\varphi_k) = 0$ for a symmetric collision, yielding

$$M_i \sinh(\varphi_i) = -\frac{e_i e_k}{2} \sinh(2\varphi_k) = -e_i e_k \gamma_k \sinh \varphi_k, \quad (101)$$

where we have used (60). Analogously, for the breaking point along trajectory k in a symmetric collision we have $\lambda_k(\varphi_i, \varphi_k) - \lambda_k(-\varphi_i, -\varphi_k) = 0$, yielding

$$M_k \sinh(\varphi_k) = -\frac{e_i e_k}{2} \sinh(2\varphi_i) = -e_i e_k \gamma_i \sinh \varphi_i, \quad (102)$$

where $\gamma_i = \cosh(\varphi_i) > 0$, showing that φ_i and φ_k must have the same sign before the collision when $e_i e_k = -1$, and we have a sticky collision. Otherwise, when $e_i e_k = 1$, Eq. (101) defines a mutual recoil where the φ 's have opposite signs. Equations (101) and (102) are linear equations relating $\sinh(\varphi_k)$ and $\sinh(\varphi_i)$, and the vanishing of the 2×2 determinant can be expressed as

$$\gamma_i / M_i = M_k / \gamma_k. \quad (103)$$

Squaring either (101) or (102), multiplying both sides by (103), and using the identity $\sinh^2(\varphi_\alpha) = \cosh^2(\varphi_\alpha) - 1 = \gamma_\alpha^2 - 1$ yields

$$M_i \gamma_i (\gamma_i^2 - 1) = M_k \gamma_k (\gamma_k^2 - 1) \equiv 2M_i M_k J, \quad (104)$$

where in the last term we have introduced the positive quantity J to parametrize both cubics. Any solution of (104) yields a solution to (101) and (102), which can easily be found with Cardano's formula. The two cubics of (104) have a single positive real root for any $J > 0$, and for sufficiently large J the solution can be approximated by

$$\gamma_i \approx M_k^{1/3} (2J)^{1/3}, \quad (105)$$

$$\gamma_k \approx M_i^{1/3} (2J)^{1/3}. \quad (106)$$

Eliminating J from (105) and (106) yields the large- J boundary layer condition

$$\gamma_k = \hbar \gamma_i, \quad (107)$$

where

$$\hbar \equiv \left(\frac{m_i}{m_k} \right)^{1/3}. \quad (108)$$

Condition (107) holds when $J \gg \frac{\hbar^{3/2}}{3\sqrt{3}}$. \square

Our next Lemma concerns symmetric collisions when $\varepsilon \neq 0$.

Lemma 5.2. *The symmetric collision $(\varphi_i, \varphi_k) \rightarrow (-\varphi_i, -\varphi_k)$ is a **sticky collision** for the electron-proton collision-at-a-distance $e_i e_k = -1$ when $|\varepsilon| < 2$.*

Proof. We are going to keep ε and ε_* in the following despite that $\varepsilon = \varepsilon_*$ when $e_i e_k = -1$, in order to refer to the formulas from outside of this lemma. Again, we start from the continuity of the left-hand side of (99) at the breaking point, i.e., $\lambda_i(\varphi_i, \varphi_k) - \lambda_i(-\varphi_i, -\varphi_k) = 0$, which yields

$$\left(M_i + \frac{\varepsilon}{2} \gamma_k \right) \sinh(\varphi_i) = -e_i e_k \left(\gamma_k - \frac{\varepsilon_*}{2} \gamma_i \right) \sinh \varphi_k, \quad (109)$$

where again we have used (60). Analogously, for the breaking point along trajectory k we have $\lambda_k(\varphi_i, \varphi_k) - \lambda_k(-\varphi_i, -\varphi_k) = 0$, yielding

$$\left(M_k + \frac{\varepsilon}{2} \gamma_i \right) \sinh(\varphi_k) = -e_i e_k \left(\gamma_i - \frac{\varepsilon_*}{2} \gamma_k \right) \sinh \varphi_i, \quad (110)$$

where $\gamma_\alpha = \cosh(\varphi_\alpha) > 0$. Equations (109) and (110) are linear equations relating $\sinh(\varphi_k)$ and $\sinh(\varphi_i)$, and the vanishing of the 2×2 determinant can be expressed either as

$$\frac{\left(\gamma_i - \frac{\varepsilon_*}{2} \gamma_k \right)}{\left(M_i + \frac{\varepsilon}{2} \gamma_k \right)} = \frac{\left(M_k + \frac{\varepsilon}{2} \gamma_i \right)}{\left(\gamma_k - \frac{\varepsilon_*}{2} \gamma_i \right)}, \quad (111)$$

or explicitly

$$\gamma_i \gamma_k = M_i M_k + \frac{\varepsilon}{2}(M_i \gamma_i + M_k \gamma_k) + \frac{\varepsilon_*}{2}(\gamma_i^2 + \gamma_k^2). \quad (112)$$

Equation (111) reduces to (103) when $\varepsilon = 0$. For $\varepsilon = \varepsilon_* < 0$, Eq. (112) requires

$$M_i M_k > \gamma_i \gamma_k. \quad (113)$$

Equations (109) and (110) with $e_i e_k = -1$ and $\varepsilon > 0$ predict a recoil when

$$\gamma_i > \frac{2\gamma_k}{\varepsilon} > \frac{4\gamma_i}{\varepsilon^2}, \quad (114)$$

which requires $\varepsilon > 2$. On the other hand, when $\varepsilon < 0$, Eqs. (109) and (110) predict a recoil for the case $e_i e_k = -1$ when

$$\gamma_i > \frac{2M_k}{|\varepsilon|} ; \quad \gamma_k > \frac{2M_i}{|\varepsilon|}, \quad (115)$$

contradicting (113) unless $\varepsilon < -2$. Therefore, the collision must be sticky if $|\varepsilon| < 2$. \square

Squaring either Eq. (109) or Eq. (110), and multiplying both sides by (111) yields

$$\left(\gamma_\alpha + \frac{\varepsilon}{4M_\alpha}(\varepsilon_* \gamma_\alpha^2 + \varepsilon M_i \gamma_i + \varepsilon M_k \gamma_k) + \frac{1}{2}(\varepsilon M_k - \varepsilon_* \gamma_k) \right) (\gamma_\alpha^2 - 1) \equiv 2J \hbar^{\mp 3/2}, \quad (116)$$

where the plus sign is for $\alpha = k$ and the minus sign is for $\alpha = i$. Equation (116) is a quartic polynomial generalizing the cubic polynomial (104) for $\varepsilon \neq 0$, which introduces a singular root, as discussed below. There is nothing wrong with a sticky collision-at-a-distance. Nevertheless, the electron-electron collision-at-a-distance continues to be a **mutual recoil** for small ε , as follows.

Lemma 5.3. *The symmetric collision-at-a-distance $(\varphi_i, \varphi_k) \rightarrow (-\varphi_i, -\varphi_k)$ must be a **mutual recoil** if $e_i e_k = 1$ and $|\varepsilon| < 2 \min(\hbar^3, \frac{1}{\hbar^3})$.*

Proof. Assuming $e_k e_i = 1$ and $\varepsilon_* = -\varepsilon$, there are two cases to consider:

1. In the case $\varepsilon > 0$, Eq. (109) accepts only mutual recoils.
2. In the case $\varepsilon < 0$, we can re-arrange Eq. (109) as

$$\frac{\sinh(\varphi_i)}{\sinh(\varphi_k)} = -\frac{2}{|\varepsilon|} \left(\frac{\gamma_k - \frac{|\varepsilon|}{2} \gamma_i}{\gamma_k - \frac{2M_i}{|\varepsilon|}} \right). \quad (117)$$

The positivity of (117) and the positivity of the respective re-arranged version of (110) requires both

$$\min\left(\frac{2M_i}{|\varepsilon|}, \frac{|\varepsilon| \gamma_i}{2}\right) < \gamma_k < \max\left(\frac{2M_i}{|\varepsilon|}, \frac{|\varepsilon| \gamma_i}{2}\right), \quad (118)$$

$$\min\left(\frac{2M_k}{|\varepsilon|}, \frac{|\varepsilon| \gamma_k}{2}\right) < \gamma_i < \max\left(\frac{2M_k}{|\varepsilon|}, \frac{|\varepsilon| \gamma_k}{2}\right). \quad (119)$$

The two alternatives are; (i) $\gamma_k > \frac{|\varepsilon|\gamma_i}{2}$ and $|\varepsilon| < 2\hbar^3$ with \hbar defined by (108) or (ii) $\gamma_i > \frac{|\varepsilon|\gamma_k}{2}$ and $|\varepsilon| < 2\hbar^{-3}$, with \hbar defined again by (108). Therefore, we have a mutual recoil until $|\varepsilon| < 2 \min(\hbar^3, \frac{1}{\hbar^3})$.

□

The velocity transformations of §7-A define a unique breaking-point-frame where the velocity of one specific particle reflects upon collision. However, one can not simultaneously control the second particle's velocity jump. For that reason, there are several inequivalent classes of collisions to be studied. We shall not study here the long list of possible collisions-at-a-distance.

6. Discussions and conclusion

1. The equation of motion (50) has a gyroscopic term (51) that is **nonlinear** and thus includes resonances as used in [3] with the provisional Chemical Principle criterion to estimate magnitudes, see also [1, 23].
2. The cubic root of the mass ratio appeared in Ref. [21] and Eq. (108). Both are applications of the Weierstrass-Erdmann conditions; Ref. [21] used variational electrodynamics to estimate of magnitudes for double-slit diffraction, see Eqs. (21) and (22) of [21], while in Eq. (108), the cubic root appeared in the boundary layer condition. Our ε -**VE** model has two parameters, (m_p/m_e) and ε , a far simpler theory than the standard model. Equations (107) and (108) predict a rough collisional boundary layer at $\left(\frac{1-v_p^2}{1-v_e^2}\right) = \left(\frac{m_p}{m_e}\right)^{2/3} \simeq 149.947$.
3. It would be helpful to repeat our studies using the full action of [9] with **two** parameters plus the electromagnetic interaction. Collisions with non-zero angular momentum should be studied as well.
4. By inspecting (66) we find that the fixed-segment of phase locking exists only for positive ε_* , which means a positive ε for the attractive case and a negative ε for the repulsive case. The former is due to the simple way functional (8) was defined here. As suggested in Ref. [9], one can re-define the original functional (8) to include an ε -strong charge q_α for each particle chosen such that $\frac{\varepsilon}{\varepsilon_*} \equiv -\frac{q_i q_j}{e_i e_j} = 1$ in the re-defined version of (8). The former has ε with the same sign for both the attractive and the repulsive cases when $\varepsilon_* > 0$. Our setup can generate several models to be studied numerically, e.g., a model for the exclusion principle, the Cooper pairs, and collisions seen in bubble chambers and particle accelerators. The subtle differences between cases should be studied numerically and used in physics to model nature. Some may differ from the standard model (or not).

5. The orbits with constant velocities of theorem 3.2 have vanishing far-fields within $\varepsilon\text{-VE}$ because the accelerations are zero, which is a strong condition to vanish far-fields. The weak condition for vanishing far-fields within pure electrodynamics requires only discontinuous velocities[27].
6. Reference [22] discusses a failed attempt to model the neutron with pure electrodynamics. An application of $\varepsilon\text{-VE}$ is to model the neutron with the fixed segments as discussed below theorem 3.2. The model should calculate the deuterium mass using a small ε to avoid perturbing electrodynamics too much. The potential accomplishment of $\varepsilon\text{-VE}$ would be an economic theory with a **single** parameter modeling the neutron **and** atomic physics [1, 3], a serious divergence-free contender for the standard model of particle physics.

7. Appendices

A. The action of the one-dimensional Lorentz group

Lorentz transformations take hyperbolas into hyperbolas, and the coordinate transformation from the synchronized clocks (t_i, x_i) of an inertial frame into the synchronized clocks (\bar{t}_i, \bar{x}_i) of another inertial frame with boost velocity $-B$ is

$$\bar{t}_i = \frac{t_i - Bx_i}{\sqrt{1 - B^2}}, \quad \bar{x}_i = \frac{x_i - Bt_i}{\sqrt{1 - B^2}}. \quad (120)$$

Notice that (120) preserves the light-cone condition, i.e., if $(t_i - t_k)^2 = (x_i - x_k)^2$ in the original frame, we also have $(\bar{t}_i - \bar{t}_k)^2 = (\bar{x}_i - \bar{x}_k)^2$ and the electromagnetic functional (8) is a Lorentz invariant. Notice that even though the light-cone condition is preserved, the distance in lightcone changes, i.e.,

$$\bar{r}_{ki}^2 = (\bar{t}_i - \bar{t}_k)^2 = \left(\frac{(t_i - t_k) - B(x_i - x_k)}{\sqrt{1 - B^2}} \right)^2 = e^{-2\varphi_B} r_{ki}^2, \quad (121)$$

where in the last equality we have introduced the boost angle by $B \equiv \tanh \varphi_B$ and used the convention of Fig. 1 that i is in the future lightcone of k , namely $(t_i - t_k) = +(x_i - x_k)$. We notice that there is no such thing as a center of mass frame in the theory of relativity, and the boost transformation is to be applied to *each* breaking point separately. As we imagine describing the collision from another frame, it is nice to express the left- and right- velocities *at* the breaking point in terms of the pre-image with a boost parameter B , as follows. The Lorentz group transforms the velocities according to

$$\bar{v}_i = \frac{v_i - B}{1 - Bv_i}, \quad (122)$$

where B is the (boost) parameter and \bar{v}_i is the image of v_i under the group action. Using definition (95), we express the boost parameter B and the velocity

\bar{v}_i as

$$B \equiv \tanh \varphi_B, \quad (123)$$

$$\bar{v}_i \equiv \tanh \bar{\varphi}_i. \quad (124)$$

Using the addition formulas for hyperbolic sines and cosines together with (59), (123) and (124), the group action translates Eq. (122) into

$$\tanh \bar{\varphi}_i = \tanh(\varphi_i - \varphi_B), \quad (125)$$

thus showing that a change of inertial frame simply shifts the velocity angle by the boost angle, i.e.,

$$\bar{\varphi}_i = \varphi_i - \varphi_B. \quad (126)$$

B. The outer-cone distances of a mutual-recoil collision

Our next result is useful in a numerical perturbation theory of the electron-electron case. We show that the mutual-recoil collision is optimal in the sense that the outer lightcone distance of each charge is much larger than the internal lightcone distance when the respective recoiling velocity is large.

Lemma 7.1. *The outer lightcone distances $r_{\beta\alpha}$ for a mutual-recoil collision are given by*

$$r_{\beta\alpha} = \frac{2}{(1 - \bar{\mathbf{v}}_\beta)} r_{k\alpha}. \quad (127)$$

Proof. Again, we assume the setup defined below (59) and further assume that particle k is in the past lightcone of particle i at time $t_i = 0$. By choosing the origin on the breaking point of particle i at time $t_i = 0$ we can extrapolate particle k 's trajectory until the future lightcone of event $(t_i, \mathbf{x}_i) = (0, 0)$ by

$$\mathbf{x}_k(t_k) = r_{ki} \hat{\mathbf{x}} + (t_k + r_{ki}) \bar{\mathbf{v}}_j,$$

where $\bar{\mathbf{v}}_j$ is the average velocity on the segment, an extrapolation valid from $t_k \geq -r_{ki}$ until the future lightcone time t_k^+ , which according to the lightcone condition happens at

$$t_k^+ = \|\mathbf{x}_k(t_k^+) - 0\| = r_{ki} + (t_k^+ + r_{ki})(\hat{\mathbf{x}} \cdot \bar{\mathbf{v}}_j),$$

yielding the future lightcone time and inverse lightcone distance to be

$$\begin{aligned} t_k^+ &= -r_{ki} + \frac{2r_{ki}}{(1 - \hat{\mathbf{x}} \cdot \bar{\mathbf{v}}_j)}, \\ \frac{1}{r_{ki}} &= \frac{(1 - \hat{\mathbf{x}} \cdot \bar{\mathbf{v}}_j)}{2r_{ki}}. \end{aligned}$$

□

C. Lagrangian extension for an external electromagnetic field

In order to include an external electromagnetic field $(E_{ext}(t, \mathbf{x}), B_{ext}(t, \mathbf{x}))$ into the equation of motion (55), one can add an external-force in the definition (42) of Λ_i^{dat} , i.e.,

$$\Lambda_i^{\text{dat}} \rightarrow \Lambda_i^{\text{dat}} + e_i \left(\mathbf{E}_{ext}(t, \mathbf{x}_i) + \mathbf{v}_i \times \mathbf{B}_{ext}(t, \mathbf{x}_i) - (\mathbf{v}_i \cdot \mathbf{E}_{ext}(t, \mathbf{x}_i)) \mathbf{v}_i \right). \quad (128)$$

The Lagrangian description of the external force is obtained by adding a linear function of each charge's velocity to the ε -strong functional (8). The oscillatory term is called the Proca Lagrangian in Ref. [16] when the external forcing is an electromagnetic wave. Notice that an external wave can exist only in the three dimensional case. As an artifact of simplified modeling, it is possible to include an external oscillatory electric field already in the one-dimensional case of Eq. (65), but the resulting motion might not display the same features of the three-dimensional case.

D. The semiflow when $\varepsilon \neq 0$ and the qualitative differences

NDDEs need a solid **segment of trajectory** to start from. In contrast, the initial condition for an ODE is the meager set made by the initial positions and initial velocities. The initial segment can have a countable number of velocity discontinuities, henceforth the photonic series associated with the segment, which is an instrumental freedom either to keep the particle bounded by exchanging velocity discontinuities in lightcone *or* to trigger further collisions. A second surprising difference is that NDDEs can have solutions with *serrated* accelerations, which are only continuous and possess no higher derivatives. In contrast, the ODEs of classical mechanics have only C^∞ solutions. Unfortunately, this complexity does not appear in Driver's problem with repulsive interaction [11], which has only C^∞ orbits, as shown below. The two-body problem with attractive interaction was studied in [8], when the present author was unaware of discontinuous velocities, and the C^∞ trajectories used in [8] all lead to head-on collisions at the speed of light. More interesting to physics and physical modeling in general, the possibility of serrated solutions is a blow to the Lorentz-Dirac equation with a renormalized mass[23, 26]. Early twentieth-century works expanded deviating arguments in power series to yield a semiflow, even at the expense of carrying a renormalized mass. The famous triple dots term of the Lorentz-Dirac equation of motion does not make sense for a serrated orbit of $C^2(\mathbb{R})$ [23, 26]. To stress that any non-zero ε makes a **qualitative** difference, we include a simple theorem on the repulsive case with $\varepsilon = 0$ [11].

Theorem 7.1. *All C^2 one-dimensional repulsive electromagnetic orbits are C^∞ .*

Proof. Electrodynamics is defined by (63) with $\varepsilon = 0$. Using Eq. (63) with $\varepsilon = 0$ and $e_i e_j = 1$ we obtain

$$\dot{\phi}_i = \frac{-1}{m_i \cosh \phi_i} \left(\frac{e^{-2\phi_j}}{2r_{ji}^2} + \frac{e^{2\phi_k}}{2r_{ki}^2} \right). \quad (129)$$

If ϕ_j and ϕ_k belong to $C^2(\mathbb{R})$, we can take another derivative of the right-hand side of (129), and thus particle i 's trajectory belongs to $C^3(\mathbb{R})$. The same is concluded from the electronic equation of motion if ϕ_s and ϕ_i are in $C^2(\mathbb{R})$, i.e., particle k 's trajectory belongs to $C^3(\mathbb{R})$ as well. Successively, ad infinitum, we show that the orbit belongs to $C^\infty(\mathbb{R})$. \square

On the other hand, when $\varepsilon \neq 0$, we can **not** take a derivative of (65) for a generic orbit of $C^2(\mathbb{R})$. The former would involve taking a derivative of past serrated accelerations on the right-hand side of (65). The same impossibility manifests in the general case, where the component $\hat{\mathcal{R}}_j \cdot \mathbf{a}_j$ of the most advanced acceleration is given in terms of past accelerations by (46). For $\varepsilon \neq 0$, the $\hat{\mathcal{R}}_j \cdot \mathbf{a}_j$ component will be a serrated function when the past data is serrated. Unlike in Driver's problem[11], serrated orbits can be solutions for one-dimensional motion with attractive interaction when $\varepsilon \neq 0$.

References

- [1] J. De Luca, *Variational Electrodynamics of Atoms, Progress In Electromagnetics Research B* **53** (2013), 147-186 (40pp).
- [2] J. De Luca, *Equations of Motion for Variational Electrodynamics, Journal of Differential Equations* **260** (2016), 5816-5833 (18pp).
- [3] J. De Luca, *Chemical Principle and PDE of Variational Electrodynamics, Journal of Differential Equations* **268** (2019), 272-300 (29pp).
- [4] J. Mallet-Paret, *Generic properties of retarded functional differential equations, Bull. Amer. Math. Soc.* **81** (1975), 750-752, J. Mallet-Paret, *Generic periodic solutions of functional differential equations, Journal of Differential Equations* **25** (1977), 163-183.
- [5] J. Mallet-Paret and R. Nussbaum, *Boundary layer phenomena for differential-delay equations with state-dependent time lags, J. Reine Angew. Math.* **477** (1996), 129-197 and *Boundary layer phenomena for differential-delay equations with state-dependent time lags-III, Journal of Differential Equations* **189** (2003), 640-692.
- [6] J. Hale, *Theory of Functional Differential Equations*, Springer-Verlag (1977), J. Hale and S. M. Verduyn Lunel *Introduction to Functional Differential Equations*, Springer-Verlag, New York (1993).
- [7] N. Guglielmi and E. Hairer, *Numerical approaches for state-dependent neutral-delay equations with discontinuities, Mathematics and Computers in Simulation* **95** (2013), 2-12 and G. Fusco and N. Guglielmi, *A regularization for discontinuous differential equations with application to state-dependent delay differential equations of neutral-type, Journal of Differential Equations* **250** (2011), 3230-3279.
- [8] E. B. Hollander and J. De Luca, *Regularization of the collision in the electromagnetic two-body problem, Physical Review E* **14** (2004), 1093-1104 (12pp).
- [9] D. J. Louis-Martinez, *Relativistic non-instantaneous action-at-a-distance interactions, Physics Letters B* **632** (2006) 733-739.

- [10] J. De Luca, *Variational principle for the Wheeler-Feynman electrodynamics*, *Journal of Mathematical Physics* **50** (2009), 062701 (24pp).
- [11] R. D. Driver, *Can the future influence the present?*, *Physical Review D* **19** (1979) 1098-1107.
- [12] J. De Luca, A. R. Humphries and S. B. Rodrigues, *Finite-element boundary value integration of Wheeler-Feynman electrodynamics*, *Journal of Computational and Applied Mathematics* **236** (2012), 3319-3337.
- [13] D. C. De Souza and J. De Luca, *Solutions of the Wheeler-Feynman equations with discontinuous velocities*, *Chaos: An Interdisciplinary Journal of Nonlinear Science* **25** (2015), 013102 (10pp).
- [14] C. M. Andersen and Hans C. von Baeyer, *Almost Circular Orbits in Classical Action-at-a-Distance Electrodynamics*, *Physical Review D* **5** (1972), 802.
- [15] G. Marmo, G. N. Mukunda, and E. C. G. Sudarshan, *Lagrangian proof of the no-interaction Theorem*, *Phys. Rev. D* **30**, 2110-2116 (1984).
- [16] J. D. Jackson, *Classical Electrodynamics*, John Wiley and Sons, New York (1975).
- [17] D. C. De Souza and M. C. Mackey, *Response of an oscillatory differential delay equation to a periodic stimulus*, *Journal of Mathematical Biology* **78** (2019) 1637-1679.
- [18] H. Shu, W. Xu, X.-S. Wang and J. Wu, *Complex dynamics in a delay differential equation with two delays in tick growth with diapause*, *Journal of Differential Equations* **269** (2020) 10937-10963.
- [19] E. B. Hollander and J. De Luca, *Two-degree-of-freedom Hamiltonian for the time-symmetric two-body problem of the relativistic action-at-a-distance electrodynamics*, *Physical Review E* **67**, 026219 (2003) (15pp).
- [20] J. Cheeger, *Differentiability of Lipschitz Functions on Metric spaces*, *GAFSA Geometric and Functional Analysis*, **9** (1999) 428-517.
- [21] J. De Luca, *Electromagnetic models to complete quantum mechanics*, *Journal of Computational and Theoretical Nanoscience* **8**, (2011) 1040-1051.
- [22] A. Schild, *Electromagnetic two-body problem*, *Phys. Rev.* **131**, (1963) 2762.
- [23] J. De Luca, *Electrodynamics of helium with retardation and self-interaction*, *Phys. Rev. Lett.* **80** (1998), 680-683 and J. De Luca, *Electrodynamics of a two-electron atom with retardation and self-interaction*, *Phys. Rev. E* **58** (1998), 5727-5741.
- [24] S.J. Aarseth and K. Zare, *A regularization of the three-body problem*, *Celestial mechanics* **10** (1974) 185-205.
- [25] A. Brault and A. Lejay, *The non-linear sewing lemma II: Lipschitz continuous formulation* *Journal of Differential Equations* **293** (2021) 482-519.
- [26] P.A.M. Dirac, *Classical theory of radiating electrons*, *Proc. Royal Society London*, **167**, 148-169 (1938).
- [27] J. De Luca, *Minimizers with discontinuous velocities for the electromagnetic variational method*, *Physical Review E* **82** (2010), 026212 (9pp).